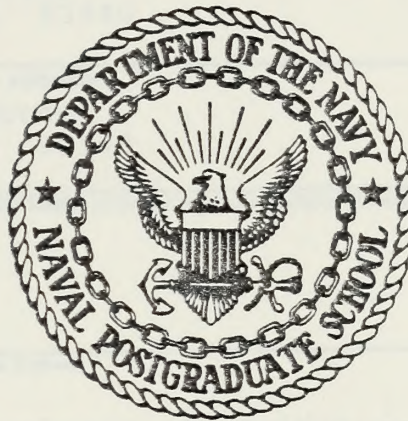


DUDLEY KNOX LIBRARY
NAVAL POSTGRADUATE SCHOOL
MONTEREY, CA 93940

NAVAL POSTGRADUATE SCHOOL

Monterey, California



THESIS

INVESTIGATION OF PIPE FLOW INSTABILITY
AND RESULTS FOR WAVE NUMBER ZERO

by

Michael James Arnold

December 1978

Thesis Advisor:

T. H. Gawain

Approved for public release; distribution unlimited.

T187434

REPORT DOCUMENTATION PAGE		READ INSTRUCTIONS BEFORE COMPLETING FORM
1. REPORT NUMBER	2. GOVT ACCESSION NO.	3. RECIPIENT'S CATALOG NUMBER
4. TITLE (and Subtitle) Investigation of Pipe Flow Instability and Results for Wave Number Zero		5. TYPE OF REPORT & PERIOD COVERED Master's Thesis; December 1978
		6. PERFORMING ORG. REPORT NUMBER
7. AUTHOR(s) Michael James Arnold		8. CONTRACT OR GRANT NUMBER(s)
9. PERFORMING ORGANIZATION NAME AND ADDRESS Naval Postgraduate School Monterey, California 93940		10. PROGRAM ELEMENT, PROJECT, TASK AREA & WORK UNIT NUMBERS
11. CONTROLLING OFFICE NAME AND ADDRESS Naval Postgraduate School Monterey, California 93940		12. REPORT DATE December 1978
		13. NUMBER OF PAGES 122
14. MONITORING AGENCY NAME & ADDRESS (if different from Controlling Office)		15. SECURITY CLASS. (of this report) Unclassified
		15a. DECLASSIFICATION/DOWNGRADING SCHEDULE
16. DISTRIBUTION STATEMENT (of this Report) Approved for public release; distribution unlimited.		
17. DISTRIBUTION STATEMENT (of the abstract entered in Block 20, if different from Report)		
18. SUPPLEMENTARY NOTES		
19. KEY WORDS (Continue on reverse side if necessary and identify by block number) Pipe Flow Instability		
20. ABSTRACT (Continue on reverse side if necessary and identify by block number) Past research by Harrison and Johnston on the stability of pipe flow yielded only tenuous results owing to errors in setup of the problem and in formulation of the complex axis boundary conditions. Recent advances in the formulation of these boundary conditions and application of generalized stability criteria allowed an accurate numerical solution to be made for angular wave number zero. The results show that flow for this case is characterized by certain		

ABSTRACT (Cont'd)

instabilities that have not been previously identified in linearized studies of this type.

A nonuniform computational mesh was developed which provided dramatic reductions in computational time on a limited basis.

Two data reduction programs were also developed to process and display data generated by the main program.

Investigation of Pipe Flow Instability
and Results for Wave Number Zero

by

Michael James Arnold
Lieutenant, United States Navy
B.S., University of Idaho, 1969

Submitted in partial fulfillment of the
requirements for the degree of

MASTER OF SCIENCE IN AERONAUTICAL ENGINEERING

from the

NAVAL POSTGRADUATE SCHOOL
December 1978

ABSTRACT

Past research by Harrison and Johnston on the stability of pipe flow yielded only tenuous results owing to errors in setup of the problem and in formulation of the complex axis boundary conditions.

Recent advances in the formulation of these boundary conditions and application of generalized stability criteria allowed an accurate numerical solution to be made for angular wave number zero. The results show that flow for this case is characterized by certain instabilities that have not been previously identified in linearized studies of this type.

A nonuniform computational mesh was developed which provided dramatic reductions in computational time on a limited basis.

Two data reduction programs were also developed to process and display data generated by the main program.

TABLE OF CONTENTS

I.	INTRODUCTION -----	9
II.	THE VORTICITY TRANSPORT EQUATION -----	12
III.	NUMERICAL METHODS -----	17
IV.	RESULTS -----	25
	A. STABILITY -----	25
	B. PERTURBATION VELOCITY PLOTS -----	27
	C. STABILITY CONTOUR PLOTS -----	28
	D. NONUNIFORM MESH EFFECTS -----	29
	E. NUMERICAL ACCURACY -----	31
V.	CONCLUSIONS AND RECOMMENDATIONS -----	46
APPENDIX A:	DERIVATION OF VORTICITY TRANSPORT EQUATION COEFFICIENTS -----	48
APPENDIX B:	FINITE DIFFERENCE EQUATIONS -----	51
APPENDIX C:	NON-UNIFORM MESH -----	57
APPENDIX D:	DERIVATION OF PERTURBATION VELOCITIES -	65
COMPUTER PROGRAMS	-----	69
LIST OF REFERENCES	-----	121
INITIAL DISTRIBUTION LIST	-----	122

LIST OF FIGURES

3-1	Finite Difference Mesh -----	18
3-2	Basic Composition of Coefficient Arrays and Vector of Unknowns -----	20
4-1	Normalized Perturbation Velocity -----	34
4-2	Normalized Perturbation Velocity -----	35
4-3	Normalized Perturbation Velocity -----	36
4-4	Normalized Perturbation Velocity -----	37
4-5	Normalized Perturbation Velocity -----	38
4-6	Stability Contour Plot -----	39
4-7	Stability Contour Plot -----	40
4-8	γ^* Versus Number of Mesh Points, N -----	41
4-9	γ^* Versus Number of Mesh Points, N -----	42
4-10	γ^* Versus Mesh Parameter, Lambda -----	43
4-11	Normalized Perturbation Velocity -----	44
4-12	Normalized Perturbation Velocity -----	45
C-1	R versus η for Four Selected Values of Lambda-Axis Offset -----	63
C-2	R versus η for Four Selected Values of Lambda-Wall Offset -----	64

TABLE OF SYMBOLS

C	Constant in non-uniform mesh functions given by equations (C-32) and (C-40)
D, D^2, \dots	Partial derivatives with respect to r .
D^*, D^{*2}, \dots	Partial derivatives with respect to η .
e	Base of natural logarithms.
$\bar{e}_x, \bar{e}_r, \bar{e}_\theta$	Unit vectors along the x , r and θ axes in cylindrical coordinates.
F, G, H	Components of the velocity vector potential defined in equation (2-6).
f_{11}, f_{22}, \dots	Coefficients of D^*Q , $D^{*2}Q$, ... in equations (C-9) through (C-12) as defined in equations (C-13) through (C-22).
i	$+\sqrt{-1}$, the imaginary unit. Also used as an index in Section III and Appendix D.
N	The number of interior points in the finite difference mesh of Section III.
O	Symbol denoting the phrase "of order".
Q	The component of the velocity vector potential derived from the component H by the change of variable, $H = rQ$.
R_e	Reynolds number based on mean velocity and pipe radius.
t	Time.
U	The streamwise velocity in Pipe Poiseuille Flow as defined by equation (2-11).
u, v, w	Components of the complex perturbation velocity defined in equation (D-1).
\bar{W}	Complex vector potential of perturbation velocity defined in equation (D-2).
x, r, θ	Cylindrical coordinates.
α	$\alpha_R + i\alpha_I$. Complex wave number of the perturbation in the x -direction.

β	in. Complex wave number of the perturbation in the θ direction, where $n = 0, 1, 2, 3, \dots$
δ	$1/(N+1)$. The r or η increment in the finite difference approximations of the derivatives of Q .
η	The independent variable replacing r in the nonuniform mesh of Appendix C.
γ	$\gamma_R + i\gamma_I$. Complex frequency of the perturbation.
$\bar{\Gamma}$	The vorticity transport equation expressed in abbreviated notation as defined in equation (2-7).
$\Gamma_x, \Gamma_r, \Gamma_\theta$	The components of $\bar{\Gamma}$ in cylindrical coordinates as defined in equation (2-7).
λ	Mesh offset parameter as defined in equations (C-32) and (C-40).
∇	Linear vector operator (nabla)
\times	Vector cross-product operator.
[]	Brackets enclosing a matrix.
{ }	Brackets enclosing a column vector.

I. INTRODUCTION

The problem of finding an analytical solution to the pipe flow stability problem has been pursued actively ever since the classical experiments of Osborne Reynolds [10] about 100 years ago. Up to now, however, no investigation has been able to satisfactorily predict flow instabilities, although many approaches have been taken.

Salwen and Grosch [11] studied pipe flow with various angular wave numbers and sinusoidal streamwise perturbations and concluded that it was stable for all axial and angular wave numbers. Perturbations with exponential growth in space but a purely sinusoidal time variation were researched by Garg and Rouleau [2] and those with both exponential growth in space and in time by Gill [3]. Both concluded that the flows were stable.

Because of this inability of linear theory to account for experimental fact, explanations by Davey and Drazin [1] involving finite disturbances and by Huang and Chen [5] and Leite [7] involving conditions at the pipe entrance have been offered. While these investigations have indeed shown instabilities to exist, a completely general solution to the linear problem has never been achieved.

Recently a more general theory was presented by Harrison [4] and further investigated by Johnston [6]. These two studies, however, failed to produce conclusive results due

to mathematical errors in the problem setup and inadequate formulation of the boundary conditions at the axis. Gawain [9] has subsequently formulated the axis boundary conditions in a new way which corrects the previous discrepancies and promises further advances.

For angular wave number, n , equal to zero, radical simplifications result in the governing equations (Section II), indicating that this case should be approached first. This investigation centers on that case.

Preliminary checks using the computer program of Ref. 6 revealed that, of the two eigenfunctions, G and H , which occur in this problem and which are uncoupled for $n = 0$, the latter appeared to be the more critical. Hence the present research was arbitrarily restricted to investigation of the stability of eigenfunction H . A similar study of the other eigenfunction, G , for $n = 0$ remains to be completed at some future time. Comparable calculations for other wave numbers ($n = 1, 2, 3, \dots$) also remain to be accomplished in the future. Extensive and systematic calculations of this type will be essential to provide the factual basis for a comprehensive theory of pipe flow stability.

Reverting to the case at hand, eigenfunction H for wave number $n = 0$, we note that the program of Ref. 6 was rewritten for this case, incorporating the newly formulated boundary conditions of Ref. 9. In addition, a new, generalized stability criteria was adopted. Moreover, a new technique was introduced which allows the use of nonuniform meshes to reduce computational time.

Lastly, two data reduction programs were written to process data produced by the main investigative program.

II. THE VORTICITY TRANSPORT EQUATION

Although a complete treatment of this subject is contained in Appendix A of Ref. 4 and further addressed in Ref. 6 and Ref. 9, it is felt that a brief overview is still required here to maintain continuity with previously referenced works. This discussion is an abbreviated version of Section II of Ref. 6.

Laminar flow of an incompressible fluid of constant viscosity is governed by the Navier-Stokes equation and the continuity equation. Taking the curl ($\nabla \times$) of the Navier-Stokes equation and introducing a perturbation velocity (\bar{v}) and vorticity ($\bar{\omega}$) gives the vorticity transport equation which is equation (A-10) of Appendix A, Ref. 4.

Expressing this equation in terms of the complex velocity vector potential, \bar{W} , gives

$$W(x, r, \theta, t) = (\bar{e}_x F(r) + \bar{e}_r G(r) + \bar{e}_\theta H(r)) e^X \quad (2-1)$$

where

$$X = \alpha x + \beta \theta + \gamma t \quad (2-2)$$

and

$$\bar{v} = \nabla \times \bar{W} \quad (2-3)$$

$$\bar{\omega} = \nabla \times \bar{v} . \quad (2-4)$$

It should also be noted that, as shown in part one of Appendix G in Ref. 4, α and γ are complex while β is a purely imaginary quantity defined by

$$\beta = i n \quad n = 0, 1, 2, \dots \quad (2-5)$$

When expressed in the form of equation (2-1), the vorticity transport equation becomes three simultaneous fourth-order differential equations of the form

$$\begin{aligned} & [M_4] \begin{Bmatrix} D^4 F \\ D^4 G \\ D^4 H \end{Bmatrix} + [M_3] \begin{Bmatrix} D^3 F \\ D^3 G \\ D^3 H \end{Bmatrix} + [M_2] \begin{Bmatrix} D^2 F \\ D^2 G \\ D^2 H \end{Bmatrix} \\ & + [M_1] \begin{Bmatrix} DF \\ DG \\ DH \end{Bmatrix} + [M_0] \begin{Bmatrix} F \\ G \\ H \end{Bmatrix} - \gamma ([N_2] \begin{Bmatrix} D^2 F \\ D^2 G \\ D^2 H \end{Bmatrix} \\ & + [N_1] \begin{Bmatrix} DF \\ DG \\ DH \end{Bmatrix} + [N_0] \begin{Bmatrix} F \\ G \\ H \end{Bmatrix}) = \begin{Bmatrix} 0 \\ 0 \\ 0 \end{Bmatrix} \end{aligned} \quad (2-6)$$

Equations (2-5) may be further expressed in the abbreviated form

$$\bar{\Gamma} = \begin{Bmatrix} \bar{\Gamma}_x \\ \bar{\Gamma}_r \\ \bar{\Gamma}_\theta \end{Bmatrix} = \begin{Bmatrix} 0 \\ 0 \\ 0 \end{Bmatrix} \quad (2-7)$$

where $\bar{\Gamma}$ appears to be a set of three coupled equations in the components of \bar{W} . As given in Appendix B of Ref. 4, equations (2-7) actually represent only two independent conditions and by an appropriate linear combination of Γ_x and Γ_θ , equations (2-6) can be expressed as a set of two equations in three unknowns. The appropriate linear combination is given in Appendix B of Ref. 4 and yields the set of equations

$$\begin{aligned} \Gamma_r &= 0 \\ -\frac{in}{r} \Gamma_x + \alpha \Gamma_\theta &= 0. \end{aligned} \quad (2-8)$$

Except for the case where n is equal to zero, equations (2-8) do not uncouple. The linear combination given by the second of equations (2-8) does, however, reduce the highest order derivative of $G(r)$ in equations (2-6) to second order. Appendix C of Ref. 4 illustrates the redundancy of the three components of \bar{W} , allowing one of these components to be arbitrarily set to zero for all r . The maximum benefits of equations (2-8) are obtained if

$$F(r) = 0 \quad (2-9)$$

Incorporating equations (2-8) and (2-9) into equations (2-6) results in the form

$$\begin{aligned}
 & [M'_4] \begin{Bmatrix} D^4_G \\ D^4_H \end{Bmatrix} + [M'_3] \begin{Bmatrix} D^3_G \\ D^3_H \end{Bmatrix} + [M'_2] \begin{Bmatrix} D^2_G \\ D^2_H \end{Bmatrix} \\
 + & [M'_1] \begin{Bmatrix} DG \\ DH \end{Bmatrix} + [M'_O] \begin{Bmatrix} G \\ H \end{Bmatrix} - \gamma ([N'_2] \begin{Bmatrix} D^2_G \\ D^2_H \end{Bmatrix} \\
 + & [N'_1] \begin{Bmatrix} DG \\ DH \end{Bmatrix} + [N'_O] \begin{Bmatrix} G \\ H \end{Bmatrix}) = \begin{Bmatrix} 0 \\ 0 \end{Bmatrix} \quad (2-10)
 \end{aligned}$$

where the coefficient matrices are given by equations (2-10) through (2-17) of Ref. 6. It is appropriate to note that these same coefficient matrices appear in Ref. 9, equations (A1) through (A9), in a slightly different form resulting from the substitutions

$$U = 2(1 - r^2) \quad (2-11)$$

$$t = \alpha^2 + \frac{\beta^2}{r^2} \quad \text{and} \quad (2-12)$$

$$T = \alpha U - \frac{1}{R_e} \left(\alpha^2 + \frac{\beta^2}{r^2} \right) . \quad (2-13)$$

As discussed in the previous section, the case where

$$\beta = \text{in} , \quad n = 0 \quad (2-14)$$

leads to great simplifications in equations (2-10), (2-12) and (2-13). In particular, equations (2-10) uncouple and allow an independent investigation of either H or G . As a result of the findings discussed in Section I, it was decided to explore the function H only. This reduced equation (2-10) to that of equation (A-6) of Appendix A, which is a linear, homogeneous fourth order differential equation in $H(r)$.

III. NUMERICAL METHODS

Substituting the change of variable $H = rQ$ as given in equation (A-1) and the coefficients defined in equations (A-11) through (A-18) into the vorticity transport relation, equation (A-6), gives the expression

$$\begin{aligned} M_4 D^4 Q + M_3 D^3 Q + M_2 D^2 Q + M_1 DQ + M_0 Q \\ - \gamma [N_2 D^2 Q + N_1 DQ + N_0 Q] = 0, \end{aligned} \quad (3-1)$$

which is a homogeneous fourth order differential equation in $Q(r)$. The boundary conditions for this case are derived in detail in Ref. 9 as

$$\begin{aligned} Q(1) &= 0 \\ DQ(1) &= 0 \\ DQ(0) &= 0 \\ D^3 Q(0) &= 0. \end{aligned} \quad (3-2)$$

The boundary finite difference equations derived in Appendix B from equations (3-2), along with the standard central difference equations given in Ref. 6, allow the function $Q(r)$ to be approximated by a finite number of discrete unknowns. As shown by Figure 3-1 below, the non-dimensionalized radius of the pipe is divided into a one-dimensional



Figure 3-1 Finite Difference Mesh

computational mesh consisting of N interior points, $N+1$ intervals, and $N+2$ total points, including the boundary points at $r = 1$ and $r = 0$. As will be discussed later, the spacing between these points may or may not be uniform. For the uniform case, the spacing is defined by

$$\delta = 1/(N+1) . \quad (3-3)$$

For the nonuniform case, a change of independent variable is performed. The spacing of the new independent variable, η , is still given by equation (3-3).

With a nonuniform mesh, the points shown in Figure 3-1 will be concentrated near the axis or near the wall according

to the type of offset specified. These effects are discussed in detail in Section IV.

Substitution of the finite difference equations of Appendix B into equation (3-1) results in a set of N , linear, algebraic difference equations in terms of the unknown value of Q at each of the N interior points of the computational mesh. Since each of these equations is of the form of a linear combination of the i th, central, point and the two, three or four adjacent points (depending on the order of the derivative being approximated), this system of equations consists of a coefficient array multiplying a vector containing the unknown value of the function Q at each of the N interior points. This technique allows the problem to be converted into an eigenvalue problem of the form

$$[X] \{Q\} - \gamma[Y] \{Q\} = 0 \quad (3-4)$$

with the basic composition of the arrays $[X]$ and $[Y]$ and the vector $\{Q\}$ as illustrated in Figure 3-2 below.

It should be noted at this point that Figure 3-2 differs somewhat from the normal finite difference banded matrix in the first two rows and last row because of the method of deriving the finite difference approximations at the boundaries. Additionally, the order of the N unknowns has been reversed from that of Ref. 6. This was done to conform to standard matrix notation.

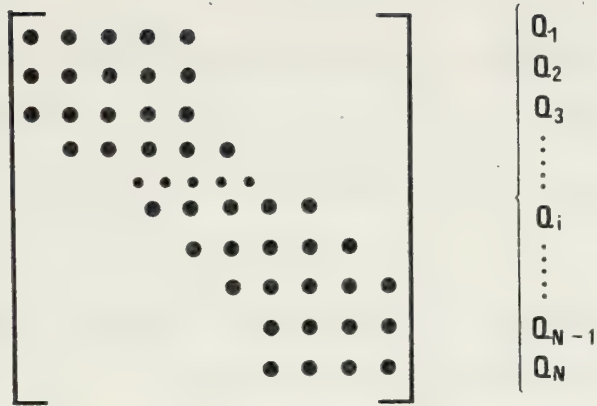


Figure 3-2 Basic Composition of Coefficient Arrays and Vector of Unknowns

This array is established by the subroutine MSET2 in conjunction with the subroutine MSET1 and function subprograms CQM1E1 and CQM2E1, which compute the numerical value for each element in the array. Subroutine MSET1 provides the coefficients given by equations (A-11) through (A-18) of Appendix A or by equations (C-24) through (C-31) if a nonuniform mesh is specified. Function CQM1E1 then computes the values for each of the elements of array $[X]$ in equation (3-4) using the coefficients passed from subroutine MSET1 in vector CQM1. Function subprogram CQM2E1 performs the same function for matrix $[Y]$ in equation (3-4) using the coefficients passed in vector CQM2.

The solution of the eigenvalue problem as formulated to this point is carried out by the controlling subroutine of program PIPE0, subroutine STAB, by the following steps:

- 1) Subroutine MSET2 is called twice to set up the coefficient matrices $[X]$ and $[Y]$ of equation (3-4).

- 2) Subroutine CDMTIN is then called to invert matrix $[Y]$, the second coefficient array in equation (3-4). CDMTIN was obtained from the IBM Library routine CMTRIN by modifying it to accept double precision arrays.
- 3) Both coefficient arrays, $[X]$ and $[Y]$, are then pre-multiplied by $[Y]^{-1}$. Since multiplication of an array by its inverse invariably results in the identity matrix, $[I]$, only the product $[Y]^{-1}[X]$ is computed using subroutine MULM. This converts the eigenvalue problem of equation (3-4) to the more conventional form

$$([Z] - \gamma[I])\{Q\} = 0 \quad (3-5)$$

where

$$[Z] = [Y]^{-1}[X] \quad (3-6)$$

- 4) Since all programs currently available for solving equations (3-5) require that the real and imaginary parts of the elements of $[Z]$ be presented in separate arrays, subroutine DSPLIT is called to accomplish this.
- 5) The eigenvalues and eigenvectors of equations (3-5) are computed using subroutines EBALAC, EHESSC, ELRH2C and EBBCKC which are available through the International

Math and Statistics Library. Subroutine EBALAC balances matrix [Z] by equalizing the exponents of all terms. The details of this transformation are retained for later use. The balanced matrix is then passed to subroutine EHSSC where it is reduced into the complex upper Hessenberg form. Subroutine ELRH2C then solves for the eigenvalues and eigenvectors. To transform the eigenvectors back into the original unbalanced form, EBBCKC is finally called using information passed from subroutine EBALAC.

For each solution, subroutine STAB determines the least stable eigenvalue (largest algebraic value) and then writes the values of N , R_e , α_R , α_I , λ , γ_{RL} , γ_{IL} and KSET to file FT02F001. The eigenvector corresponding to the least stable eigenvalue is also written to FILE FT02F001 when MODENO is set equal to one.

Control of subroutine STAB is accomplished by the main program, PIPE0. This program is a time-sharing (CP/CMS) program. Modes one and three compute the stability of the flow for a given set of input conditions. Mode one writes the least stable eigenvector to FILE FT02F001 while this output is inhibited when MODENO is set equal to three. To generate data for program EIGFCN, program PIPE0 must be run with MODENO equal to one.

Mode two operation generates a grid of stability values (stability map) based on parameters read in from FILE FT01F001. Due to the long run time in this mode, only small meshes can be generated under CP/CMS. Longer runs must be accomplished under batch, with changes to the program as specified in the comments section. Data is output to file FT03F001 when MODENO is equal to two and is compatible with program STBCONT.

The plotting programs EIGFCN and STBCONT were used to process the data generated by program PIPE0 in modes one and three, respectively. Program EIGFCN generates normalized plots of the perturbation velocity, u , as a function of radius, r . The perturbation velocities generated in accordance with Appendix D were normalized in two steps. First the perturbation velocity of largest magnitude was determined. Letting this velocity be termed u_C , a normalizing constant producing unit magnitude and zero phase angle in u_C was found in the following manner:

If

$$u_C = u_{RC} + iu_{iC} , \quad (3-7)$$

then

$$Cu_C = 1 + i(0) \quad (3-8)$$

where C is the normalizing constant. Thus,

$$C = \frac{1}{u_{RC} + iu_{iC}} = \frac{u_{RC} - u_{iC}}{(u_{RC}^2 - u_{iC}^2)} \quad (3-9)$$

$$= \frac{\bar{u}_C}{|u_C|^2} \quad (3-10)$$

where \bar{u}_C is the complex conjugate of u_C .

The nondimensionalized radius values were taken directly from the data cards for uniform meshes or computed from equations (C-32) or (C-40) in the case of a nonuniform mesh.

Program STBCONT plots the stability contours against α_R and α_I . The stability map generated by program PIPE0 is searched columnwise and rowwise for sign changes for each of the three stability criteria discussed in Section V and Ref. 9. The points are then plotted, producing contours of incipient, critical and fully developed instability and areas that denote stable flow and subcritical, supercritical and hypercritical instability.

Both programs, EIGFCN and STBCONT, utilize the NPS VERSATEC plotter, certain built-in VERSATEC subroutines, and subroutine PLOTG. These routines are only accessible when running under FORTCLGW.

IV. RESULTS

A. STABILITY

Since an understanding of the term stability is necessary to interpret the results of this investigation, a brief discussion is presented here. A complete discussion of the generalized criteria of stability is given by Gawain [9].

The characteristics of the flow for the case $n = 0$ are set by the parameters R_e and α . For fixed values of these parameters, the solution of equations (3-5) is a set of N eigenvalues, γ , and their corresponding eigenvectors, Q . As can readily be seen from equation (2-1), the value of the real part of the complex eigenvalue γ will determine the growth or decay rate in time of the perturbation. Since positive values of the real part of γ represent an exponential growth rate in time, the most important γ is the one having the largest algebraic value for its real part. This root is termed the least stable root and will be represented by the symbol γ_{RL} . As the stability represented by γ_{RL} is that seen by a fixed observer, it is not the most general criterion. As derived in Ref. 9, a more appropriate stability criterion is that based on an axis system moving at the average volumetric velocity of the flow. This criteria is termed γ_{RL}^* and is defined by Ref. 9 as

$$\gamma_{RL}^* = \gamma_{RL} + \alpha_R . \quad (4-1)$$

For this and subsequent discussions, the subscript will be dropped and γ^* will refer to the quantity defined by equation (4-1). Three stability cases arise from this equation. The first is termed incipient instability and is defined by

$$\gamma^* = -|\alpha_R| . \quad (4-2)$$

The second case, termed critical instability, is given by

$$\gamma^* = 0 \quad (4-3)$$

and, lastly, the case termed fully developed instability is said to exist when

$$\gamma^* = +|\alpha_R| . \quad (4-4)$$

The transition from stable flow to fully developed instability is progressive and several distinct stages are given in Ref. 9 to describe this transition. The region from incipient to critical instability is termed subcritical instability, that from critical instability to fully developed instability is called supercritical instability while that beyond fully developed instability is termed hypercritical instability.

B. PERTURBATION VELOCITY PLOTS

Initial investigation of the function Q was centered around plotting its appearance in the region of interest. A Reynolds number of 1150 (2300 based on diameter) was chosen as this value is generally accepted as the nominal value for transition to turbulent flow. The value of α was set at $-0.5 + i 10.0$ for the major part of the investigation as preliminary checks revealed that supercritical instabilities were present for this value. A secondary Reynolds number of 4000 was chosen to show trends.

The quantity chosen as the most realistic and representative of the eigenfunction Q is the axial perturbation velocity, u . This quantity was derived from the elements of the least stable eigenvector as outlined in Appendix D. Initially, R_e and α_I were held fixed and α_R was varied over a range of positive and negative values. For values of α_R below about two, the normalized perturbation velocity was found to have all activity near the axis with a decay essentially to zero by $r = 0.3$. A typical plot of u versus r for an α_R in this range is shown in Figure 4-1. When α_R was made sufficiently positive, the plot changed significantly in both appearance and region of activity. Figure 4-2 shows a plot of u for $\alpha_R = 2.5$. The activity can now be seen to be concentrated near the wall, with most of the activity occurring at r values greater than 0.7.

Although no particular relationship between the nature of u and the stability of the flow was evident or expected,

the plots were nevertheless valuable as indicators for various parameters involved in the investigation.

First, as can be seen by the differences in Figures 4-1 and 4-2, the plots were ideal indicators of changes in the nature of the function Q . Secondly, the adequacy of the mesh could be directly observed by noting the number of points defining the curves in regions of high activity. Figures 4-3, 4-4 and 4-5 show the same conditions as Figure 4-1 but with decreasing number of mesh points, N . Lastly, the effects of nonuniform meshes could be observed as will be discussed later in this section.

C. STABILITY CONTOUR PLOTS

The principal results of this investigation are shown in Figures 4-6 and 4-7. Although these two figures pertain to only a limited portion of the complex α plane, they do represent a significant advance in the investigation of pipe flow stability. As can be seen in these figures, the flow is characterized by regions of differing stability, ranging from stable through supercritical instability. Note that these two figures correspond to Reynolds numbers of 1150 and 4000, respectively. This is a result that has not, to this writer's knowledge, been heretofore achieved by a linearized analysis of fully developed pipe flow. The figures also show that, as has been born out by previous investigations, flow for purely sinusoidal oscillations ($\alpha_R = 0$) is stable. Additionally, a comparison of Figures 4-6

and 4-7 shows the effect of Reynolds number on the flow stability. It is clear from this comparison that an increase in Reynolds number reduces the size of the stable regions in the complex α plane; in other words, stability decreases with increasing Reynolds number. This trend agrees with our general experience pertaining to fluid flow. Lastly, the effect of the real and imaginary parts of the wave number α can readily be seen. For α_R , increasingly negative values produce successively greater levels of instability. While a contour plot was not produced for positive values of α_R , point checks of stability in this region suggest that somewhat similar contours exist in the right half-plane also. For α_I , increasing values produce increasing stability. This effect is also more pronounced at the lower Reynolds number.

D. NONUNIFORM MESH EFFECTS

One of the difficulties in this investigation was the relatively long computing time required to obtain an accurate solution, especially when operating under CP/CMS (time-sharing). The major factor controlling computing time was the number of interior mesh points, N . As an example, an increase in N of 50 percent resulted in a fourfold increase in computing time. Therefore, the desired objectives of rapidity and accuracy were in direct conflict. Additionally, follow-on investigations for values of angular wave number n other than zero involve matrices twice the order required for this case because of the coupling of equations (2-8).

For these reasons, a nonuniform mesh was developed to obtain increased accuracy at lower values of N . The nature of the velocities as seen in Figures 4-1 and 4-2 shows that a high degree of resolution in the computational mesh is only required in the vicinity of the axis (α_R less than about 2) or the wall (α_R greater than about 2). It was therefore theoretically possible to redistribute the points at moderate values of N to attain resolutions equivalent to much finer (and more time-consuming) uniform meshes.

As can be seen from Figures 4-8 and 4-9, the value of γ^* varies with the number of mesh points, N . Theoretically, each of these curves would approach some limiting value if N were increased without bound, and it is this theoretical limit that represents the required solution. In practice, it is adequate to approximate the unknown limit by a point that lies on the relatively flat portion of the curve at a value of N which is practically attainable and which does not involve a prohibitively long computing time. It has been found in this investigation that $N = 79$ fulfills these conditions.

The conversion to a nonuniform mesh involved a change of independent variable and the introduction of an analytical function to control the distribution of the mesh points. The details of these steps are given in Appendix C. By varying the mesh offset parameter, λ , it was possible to vary γ^* over a wide range. To determine when the high

accuracy solution ($N = 79$) and the nonuniform solutions were approximately equal, γ^* was plotted versus λ for fixed values of R_e , α and N with the value of γ^* for $N = 79$ as a reference. Figure 4-10 shows a plot of this type for $N = 31$. The appropriate value of λ can be seen to be approximately 1.1. Figure 4-11 is the perturbation velocity plot of the solution for $N = 31$ and $\lambda = 1.1$ for the same R_e and α as Figure 4-1. Note that the γ^* values are equal for these two figures. While the resolution of Figure 4-11 is not quite as fine as that of Figure 4-1, a comparison of Figure 4-11 with Figure 4-5 makes the improved resolution obvious. Figures 4-2 and 4-12 are similar to Figures 4-1 and 4-11 except that a wall offset was used. Note that for this case $\lambda = 1.2$, which points to a drawback of the nonuniform mesh, that of dependence on input conditions. While a check of λ dependence on α was not made, it most probably exists. There is also, however, the possibility that for small regions of the complex α plane, the variations in λ are small enough to allow an average value of λ to be nearly optimum for the entire region. While not used for the main results of this study, the method as developed here may well prove to be of maximum utility in follow-on investigations of higher angular wave numbers.

E. NUMERICAL ACCURACY

To ensure that the solutions presented here were of sufficient accuracy, two separate checks were made. The

first, γ^* dependence on N , is the most commonly used criterion.

For a solution to be accurate, it should be virtually independent of mesh fineness, that is, of N . The required magnitude of N for an accurate solution was found by plotting γ^* against N . Figures 4-8 and 4-9 both show that the solution is well converged for $N = 79$ at Reynolds numbers of 1150 and 4000, as γ^* changes by only .001 to .003 from $N = 31$ to $N = 79$ for both values of Reynolds number.

The second verification of the solution, so obvious that it is sometimes overlooked, involves simply substituting the numerical solution (least stable eigenvector) into the governing equation to ensure that it is indeed being satisfied. A short program was independently written to check the finite difference representations of equation (3-1) at the first and last interior stations and at a mid-radius station. Initial checks of numerical solutions yielded unsatisfactory results and led to the discovery of various programming errors. In particular, it was discovered that four double precision constants in the finite difference approximations were lacking the required "D0" exponent. Elimination of these seemingly trivial errors resulted in a surprising four order-of-magnitude improvement in the accuracy of the solution, with the left side of equation (3-1) improving from order 10^{-4} to order 10^{-8} .

It is instructive to note at this point that the order of magnitude of the left side of equation (3-1) is not the

true measure of its satisfaction. A more correct procedure is to compare this value with the largest term in the equation. When examined from this viewpoint, the relative error for solutions at $R_e = 1150$ and $R_e = 4000$ are found to be of order 10^{-11} to 10^{-12} , a very satisfactory result.

Therefore, by these results, the solutions presented here are both virtually independent of N and satisfy the governing differential equation to a high degree. The efforts expended to reach these conclusions were well worth the result and also point out that attention to detail is fundamental to accurate numerical results.

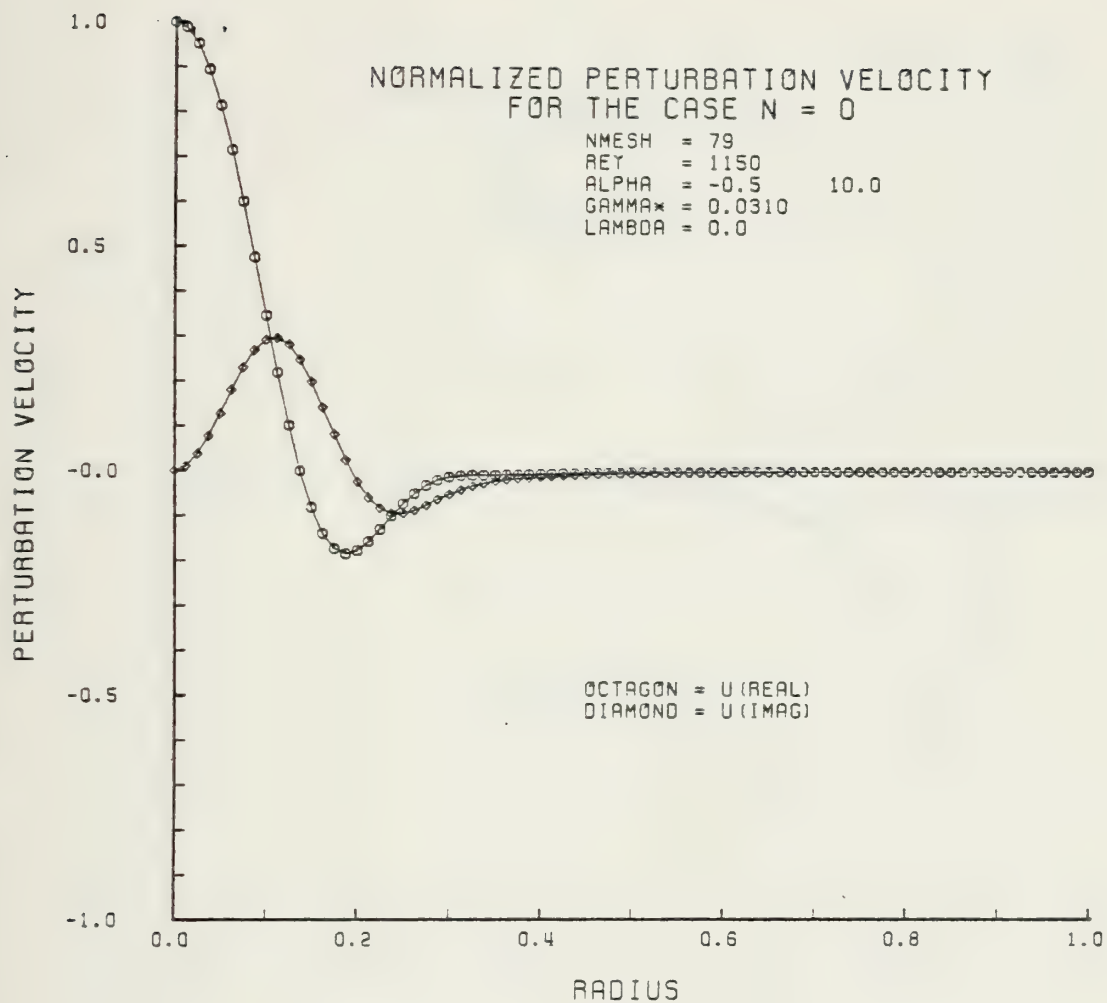


FIGURE 4-1

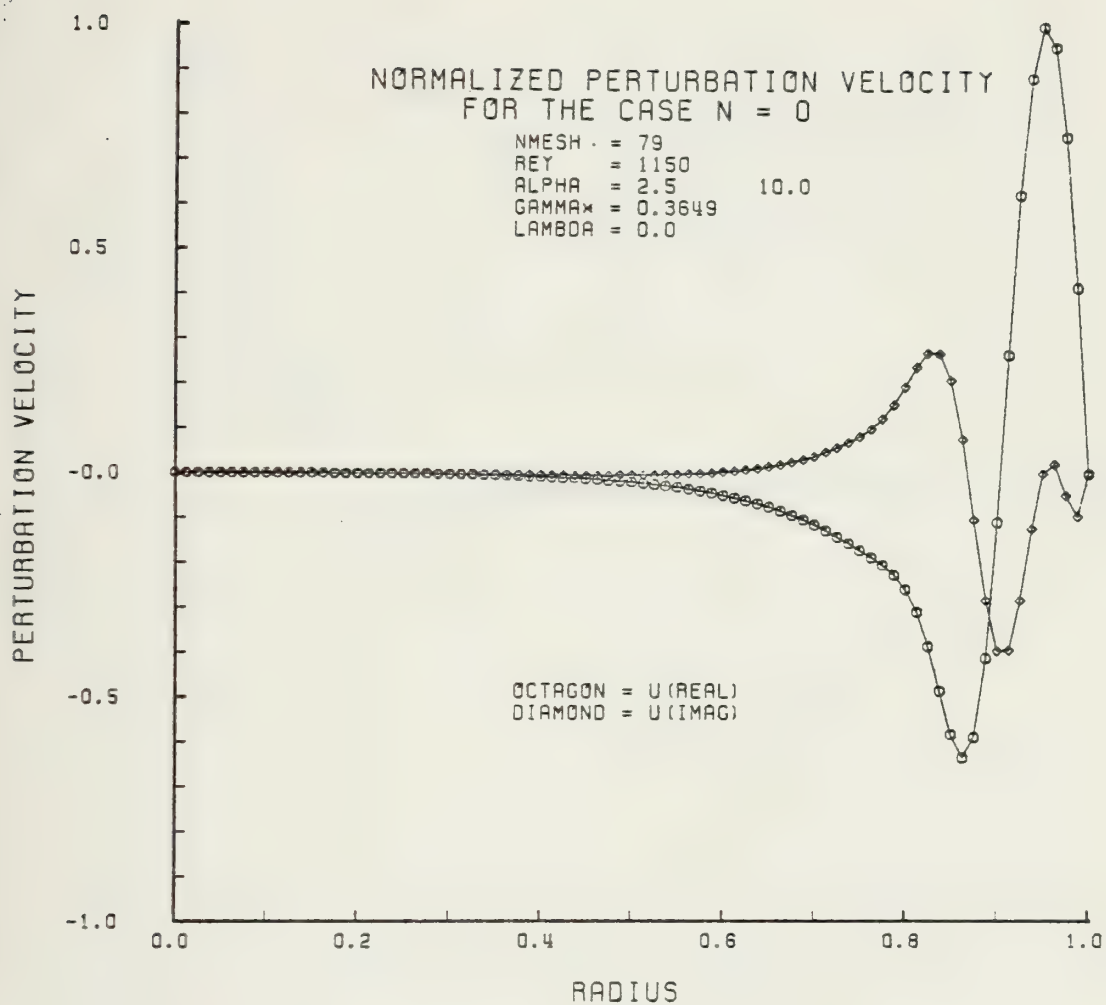


FIGURE 4-2

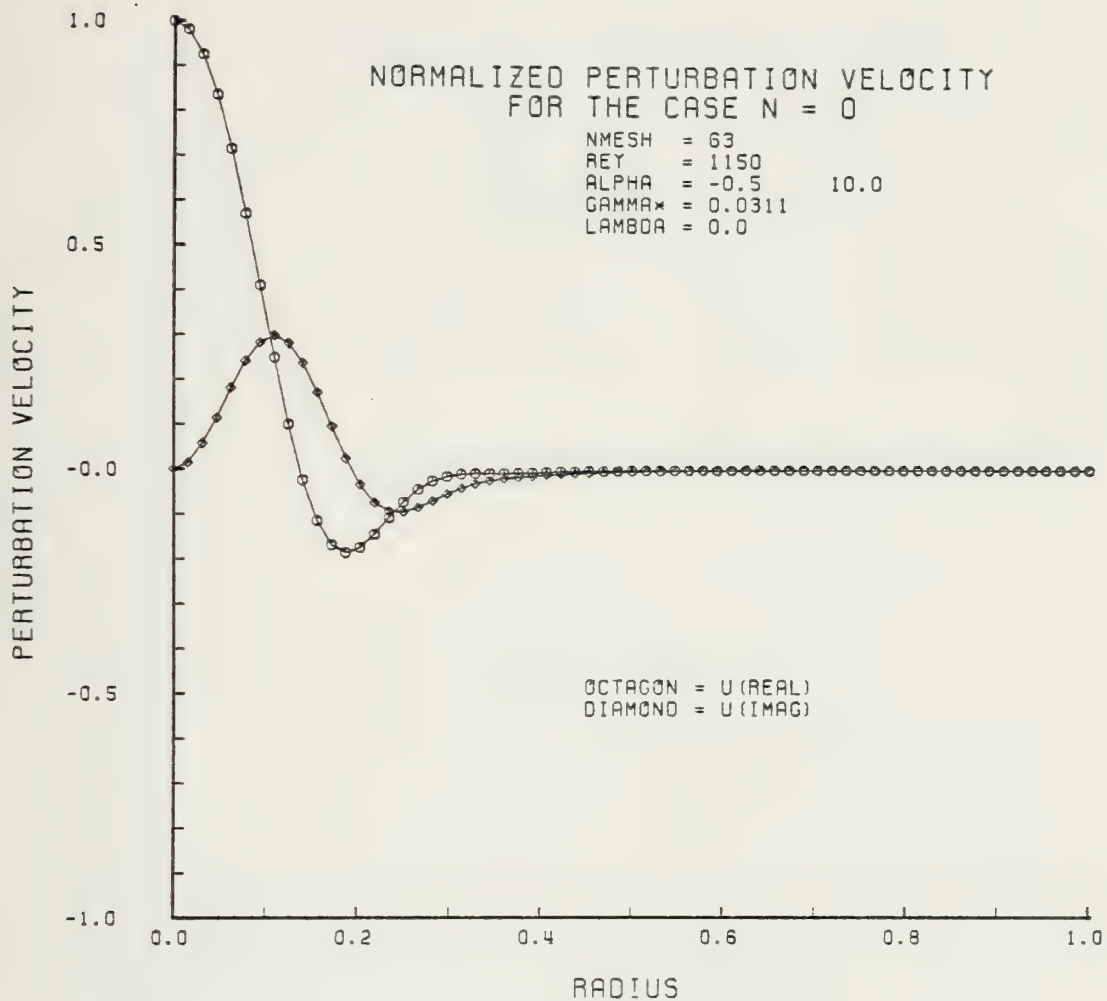


FIGURE 4-3

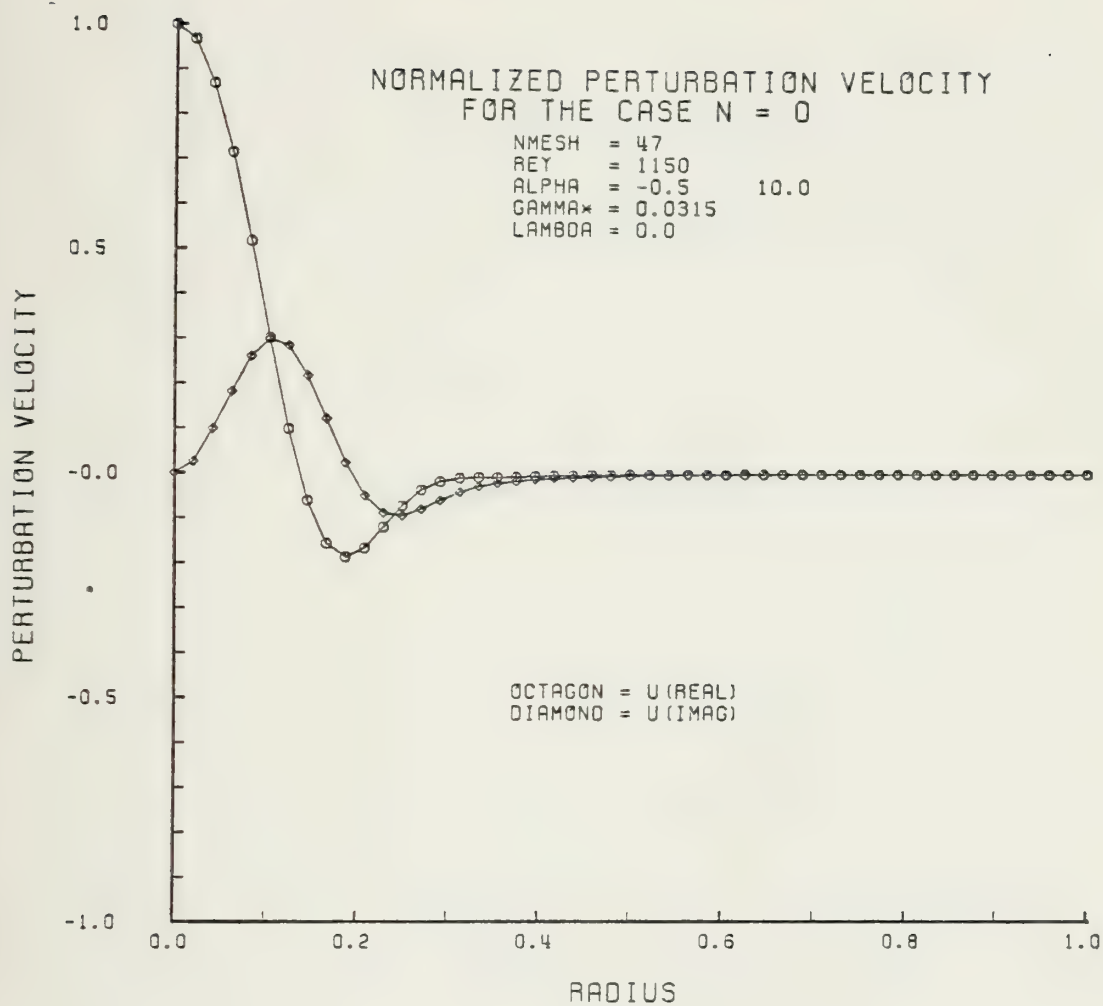


FIGURE 4-4

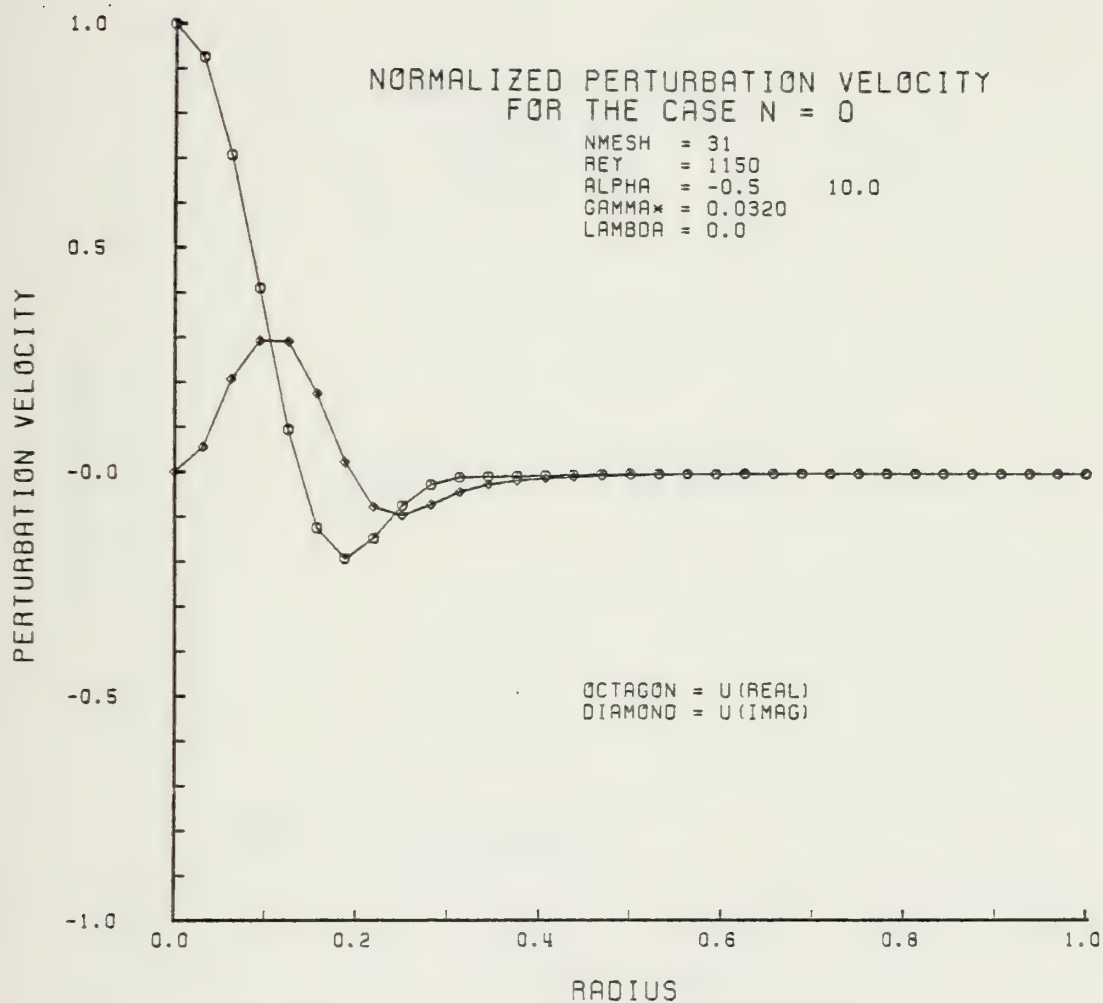


FIGURE 4-5

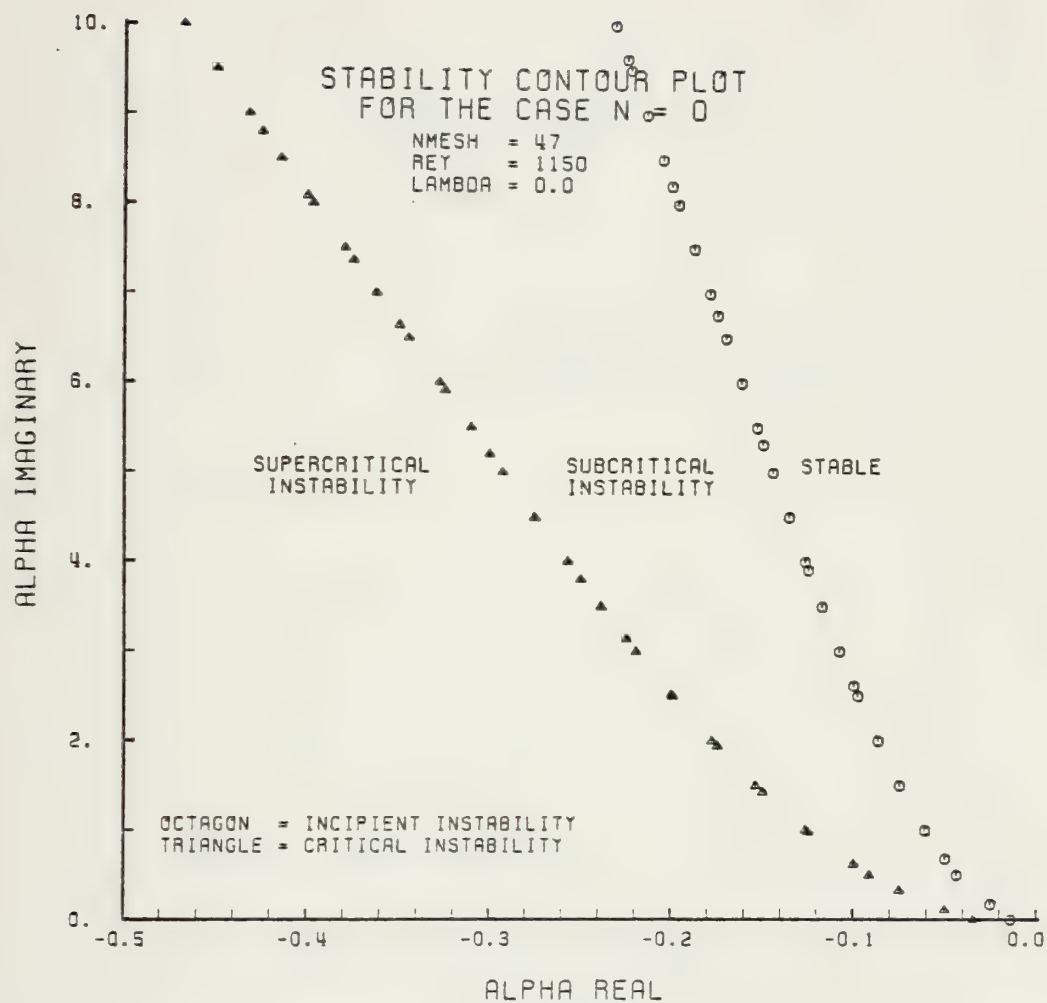


FIGURE 4-6

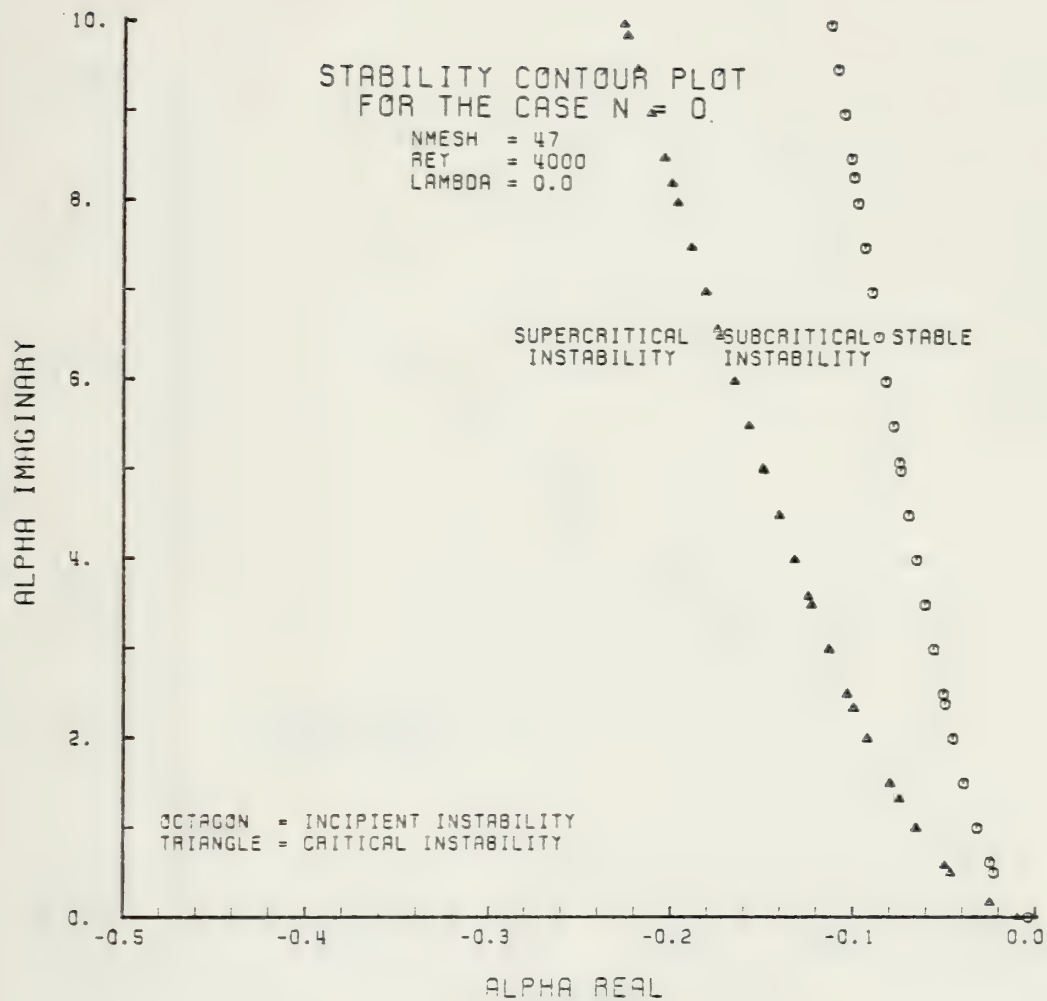


FIGURE 4-7

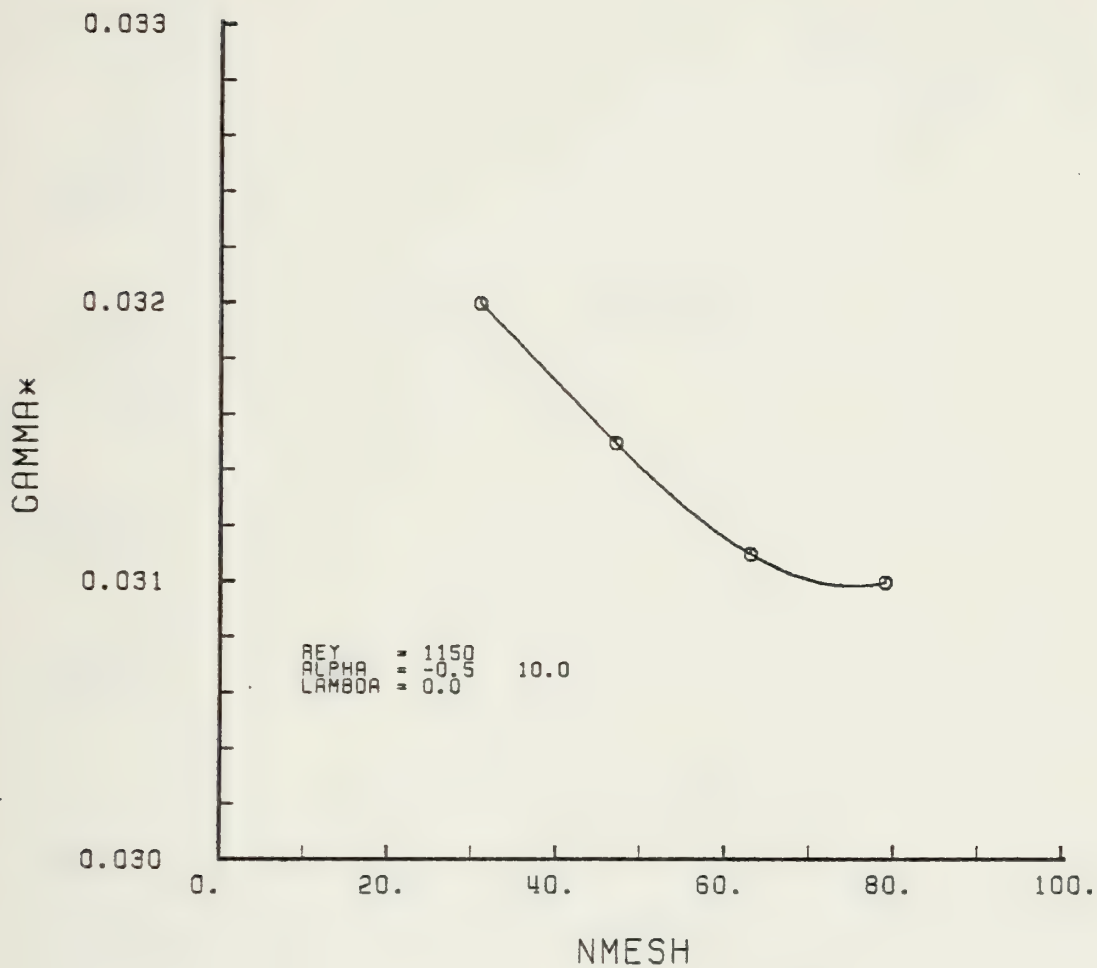


FIGURE 4-8. γ^* Versus Number of Mesh Points, N.

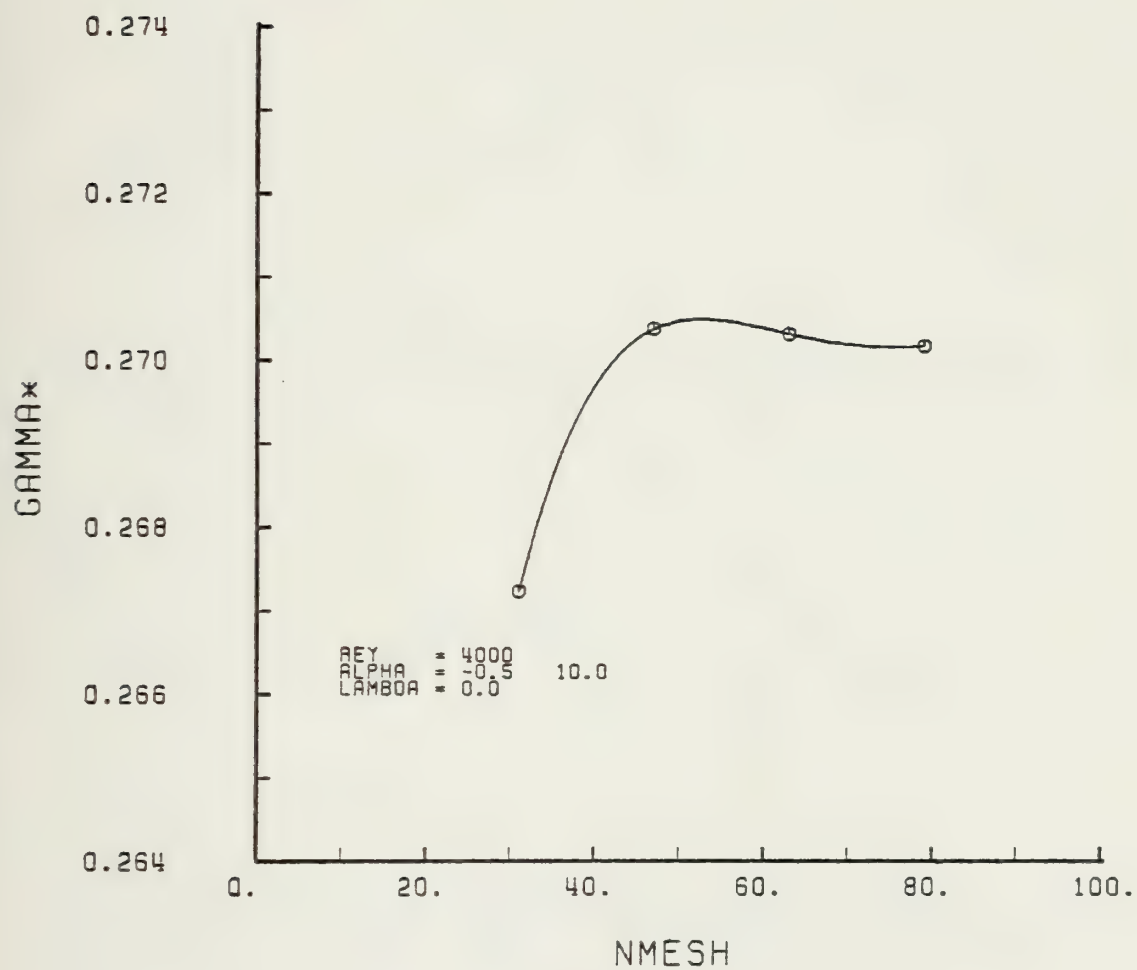


FIGURE 4-9. γ^* Versus Number of Mesh Points, N.

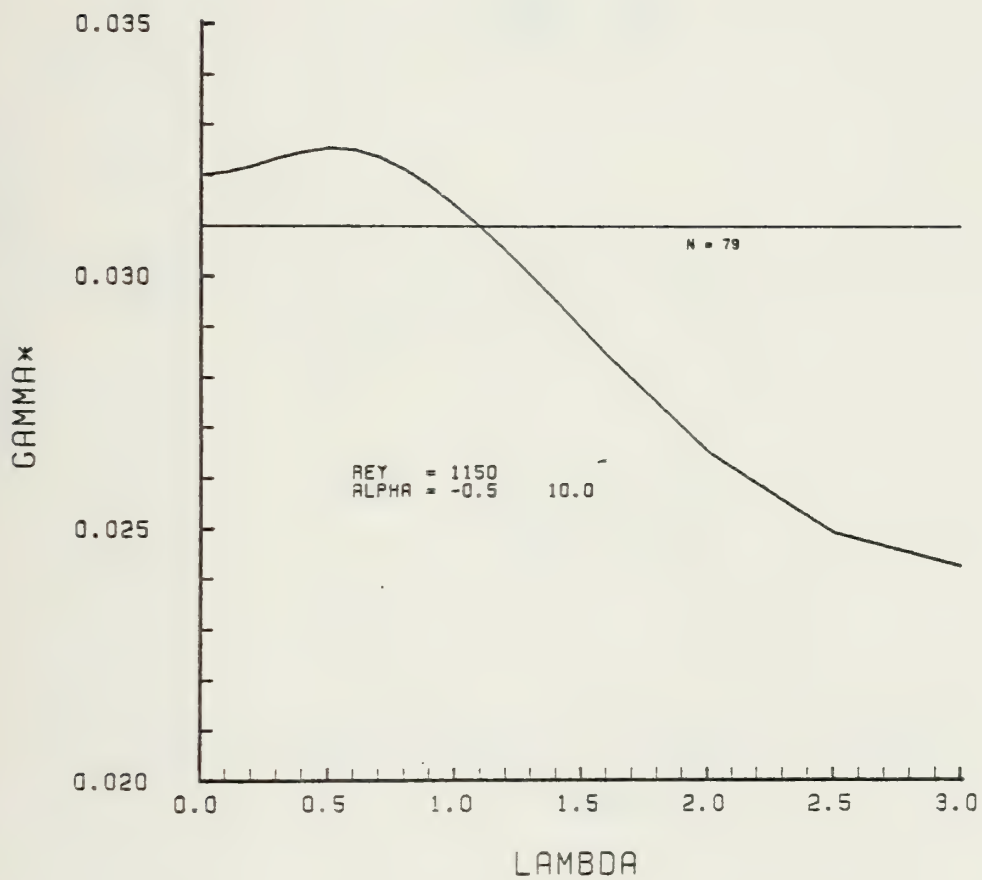


FIGURE 4-10. γ^* Versus Mesh Parameter, Lambda

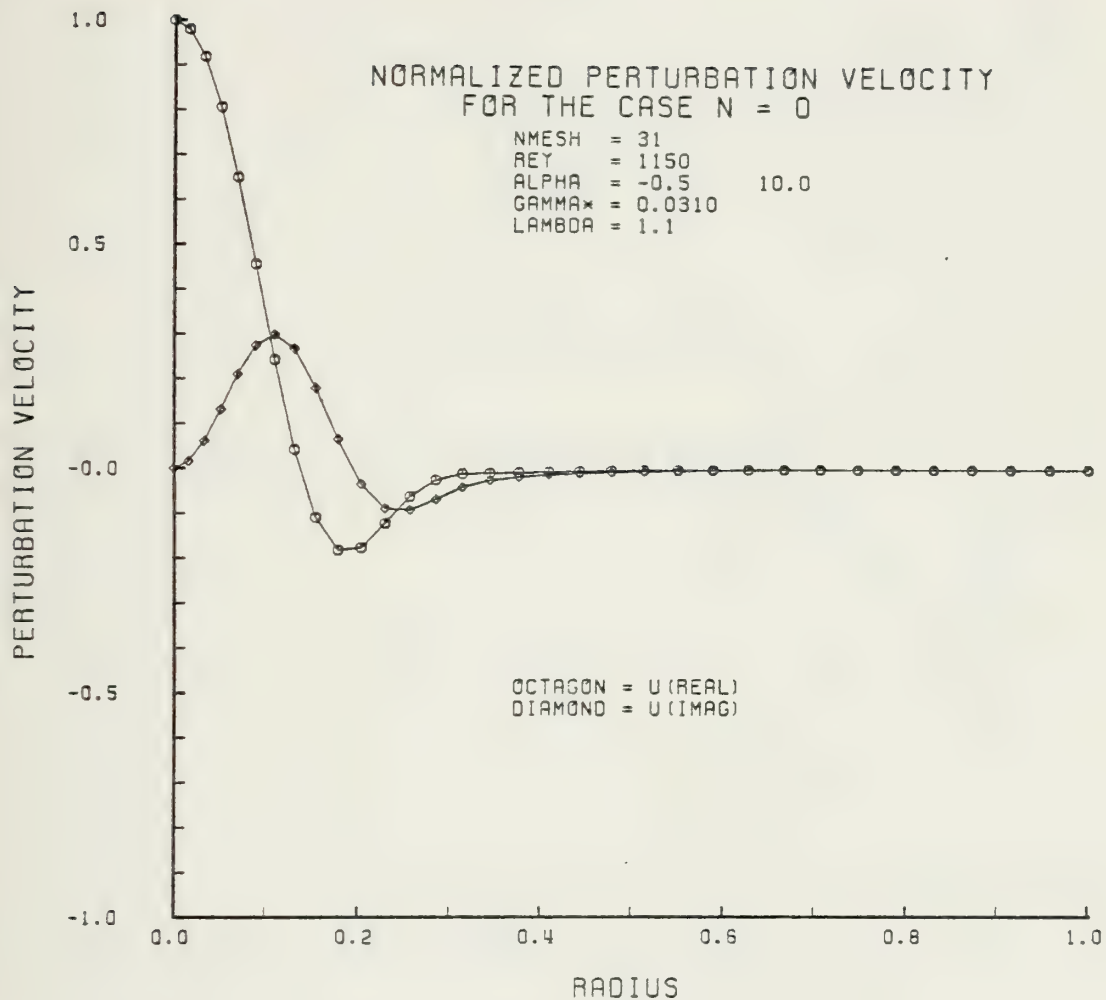


FIGURE 4-11

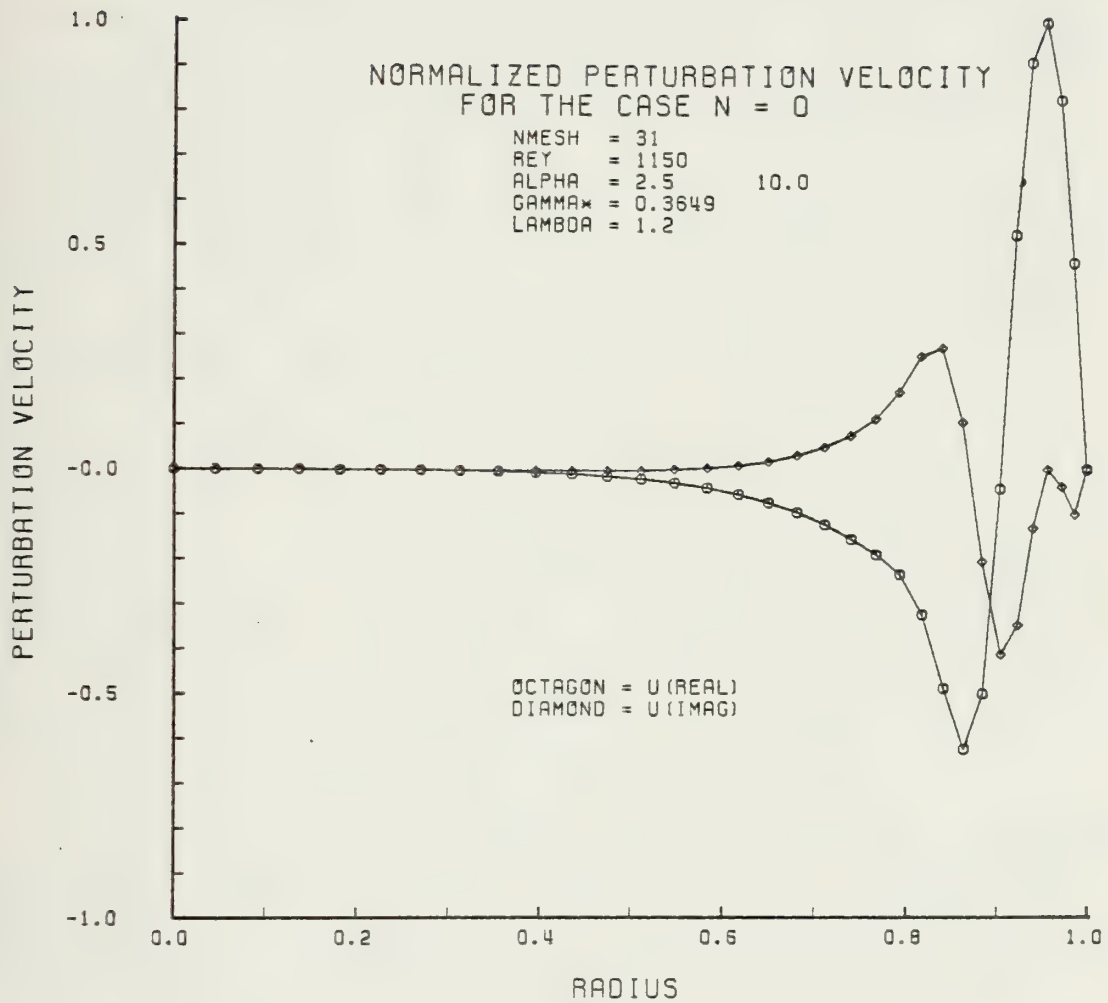


FIGURE 4-12

V. CONCLUSIONS AND RECOMMENDATIONS

The implementation of the newly developed boundary conditions of Gawain [9] has permitted a stable, numerical solution to the linearized vorticity transport equation. The results of the numerical solution are presented in Section IV and show that the stability of pipe Poiseuille flow is governed by the three parameters, α_R , α_I and R_e . In particular, both positive and negative values of α_R , that is, streamwise growth and decay in space, if sufficiently large, produce unstable growth rates in time. This result is new and it is consistent with the known experimental fact that transition to turbulent flow depends not only on Reynolds number but also on the general character of the perturbations which exist in the flow.

The perturbation velocity plots of Section IV represent the first practical look at the function Q . These plots were valuable indicators for adequacy of mesh fineness, that is, N , changes in the nature of the function Q and effects of a nonuniform mesh.

No instabilities were discovered for purely sinusoidal perturbations ($\alpha_R = 0$). This is consistent with the previous investigation of Ref. 11, but should not be assumed for investigations of other angular wave numbers, ($n = 1, 2, 3, \dots$).

Adequate numerical accuracy was proven by demonstrating that the solution was virtually independent of the number of mesh points, N , and that it satisfied to a high degree an independent check of the governing differential equation. This procedure should also be carried out in future investigations prior to conducting full scale data runs.

This study suggests that similar, and perhaps even more rewarding results will be obtained for the higher angular wave numbers. Although lengthy, programming is straightforward if approached systematically. The general organization of the programs of Ref. 4 or Ref. 6 should be helpful in this task. It is recommended that the case for $n = 1$ be undertaken as a follow-on to this study.

The nonuniform computational mesh was shown to be a powerful tool in the reduction of computational time. At the same time, however, the dependence of the mesh offset parameter, λ , on input conditions needs to be investigated further to realize the full potential of this technique.

APPENDIX A

DERIVATION OF VORTICITY TRANSPORT EQUATION COEFFICIENTS

From the change of variable introduced in Ref. 9, the function H for the case $n = 0$ is expressed by

$$H = rQ \quad (A-1)$$

Taking derivatives

$$DH = rDQ + Q \quad (A-2)$$

$$D^2H = rD^2Q + 2DQ \quad (A-3)$$

$$D^3H = rD^3Q + 3D^2Q \quad (A-4)$$

$$D^4H = rD^4Q + 4D^3Q \quad (A-5)$$

Let the '*' superscript denote element (2,2) of matrices (A1) through (A9) of Ref. 9. Since for $n = 0$, only the function H was investigated, equations (2-10) become

$$\begin{aligned} M_4^* D^4H + M_3^* D^3H + M_2^* D^2H + M_1^* DH + M_0^* H \\ - \gamma [N_2^* D^2H + N_1^* DH + N_0^* H] = 0 \end{aligned} \quad (A-6)$$

Substituting for H, equation (A-6) becomes

$$\begin{aligned}
& M_4^* \{rD^4Q + 4D^3Q\} + M_3^* \{rD^3Q + 3D^2Q\} + M_2^* \{rD^2Q + 2DQ\} \\
& + M_1^* \{rDQ + Q\} + M_0^* \{rQ\} - \gamma [N_2^* \{rD^2Q + 2DQ\} \\
& + N_1^* \{rDQ + Q\} + N_0^* \{rQ\}] = 0
\end{aligned} \tag{A-7}$$

Before proceeding further, it should be noted that the Ref. 9 matrices from which the coefficients for equation (A-7) were taken were obtained from matrices (2-10) through (2-17) of Ref. 6 by means of the following substitutions:

$$U = 2(1 - r^2) \tag{A-8}$$

$$t = \alpha^2 \frac{n_2}{r^2} \tag{A-9}$$

$$T = \alpha U - \frac{1}{R_e} \left(\alpha^2 - \frac{n_2}{r^2} \right) \tag{A-10}$$

Defining the new coefficients for equation (A-7) as M_0 through M_4 and N_0 through N_2

$$M_4 = rM_4^* = -\frac{r}{R_e} \tag{A-11}$$

$$M_3 = 4M_4^* + rM_3^* = -\frac{6}{R_e} \tag{A-12}$$

$$M_2 = 3M_3^* + rM_2^* = r\alpha U - \frac{1}{R_e} \left\{ \frac{3}{r} + 2\alpha^2 r \right\} \tag{A-13}$$

$$M_1 = 2M_2^* + rM_1^* = 3\alpha U + \frac{3}{R_e} \left\{ \frac{1}{r^2} - 2\alpha^2 \right\} \tag{A-14}$$

$$M_0 = M_1^* + rM_0^* = r\alpha^3 U - \frac{\alpha^4 r}{R_e} \tag{A-15}$$

$$N_2 = rN_2^* = -r \quad (\text{A-16})$$

$$N_1 = 2N_2^* + rN_1^* = -3 \quad (\text{A-17})$$

$$N_0 = N_1^* + rN_0^* = -\alpha^2 r \quad (\text{A-18})$$

Upon making use of the foregoing substitutions, the governing relation can finally be reduced to the form previously shown in equation (3-1).

APPENDIX B

FINITE DIFFERENCE EQUATIONS

Improved finite difference equations for the boundaries were obtained by not using the virtual point method of Ref. 4 and Ref. 6 and deriving the forms directly from the boundary conditions of Appendix A. The equations thus formed are also of consistent order truncation error, significantly improving the accuracy of the solution [Ref. 8].

Because of a peculiarity in the form of the consistent second order truncation error equations at the axis, a singularity resulted for α equal to zero. Consistent third order truncation error equations eliminated this problem.

From Appendix A, the axis boundary conditions are

$$DQ(0) = 0 \quad \text{and} \quad D^3Q(0) = 0 \quad (\text{B-1})$$

Representing Q by a power series and applying equations (B-1) yields

$$\begin{aligned} Q(r) = & Q(0) + D^2Q(0)\frac{r^2}{2!} + D^4Q(0)\frac{r^4}{4!} + D^5Q(0)\frac{r^5}{5!} \\ & + D^6Q(0)\frac{r^6}{6!} + \dots \end{aligned} \quad (\text{B-2})$$

Using five mesh points at $r = \delta, 2\delta, 3\delta, 4\delta$ and 5δ results in the matrix

$$\begin{bmatrix} Q_1 \\ Q_2 \\ Q_3 \\ Q_4 \\ Q_5 \end{bmatrix} = \begin{bmatrix} 1 & \frac{1}{2} & \frac{1}{24} & \frac{1}{120} & \frac{1}{720} \\ 1 & 2 & \frac{16}{24} & \frac{32}{120} & \frac{64}{720} \\ 1 & \frac{9}{2} & \frac{81}{24} & \frac{243}{120} & \frac{729}{720} \\ 1 & 8 & \frac{256}{24} & \frac{1024}{120} & \frac{4096}{720} \\ 1 & \frac{25}{2} & \frac{625}{24} & \frac{3125}{120} & \frac{15625}{720} \end{bmatrix} \begin{bmatrix} Q(0) \\ \delta^2 D^2 Q(0) \\ \delta^4 D^4 Q(0) \\ \delta^5 D^5 Q(0) \\ \delta^6 D^6 Q(0) \end{bmatrix} + O\delta^7$$

(B-3)

Differentiating equation (B-2) and substituting $r = \delta$ gives
(in matrix form)

$$\begin{bmatrix} Q(\delta) \\ \delta D Q(\delta) \\ \delta^2 D^2 Q(\delta) \\ \delta^3 D^3 Q(\delta) \\ \delta^4 D^4 Q(\delta) \end{bmatrix} = \begin{bmatrix} 1 & \frac{1}{2!} & \frac{1}{4!} & \frac{1}{5!} & \frac{1}{6!} \\ 0 & 1 & \frac{1}{3!} & \frac{1}{4!} & \frac{1}{5!} \\ 0 & 1 & \frac{1}{2!} & \frac{1}{3!} & \frac{1}{4!} \\ 0 & 0 & 1 & \frac{1}{2!} & \frac{1}{3!} \\ 0 & 0 & 1 & 1 & \frac{1}{2!} \end{bmatrix} \begin{bmatrix} Q(0) \\ \delta^2 D^2 Q(0) \\ \delta^4 D^4 Q(0) \\ \delta^5 D^5 Q(0) \\ \delta^6 D^6 Q(0) \end{bmatrix} + O\delta^7$$

(B-4)

Let [A] and [B] denote the coefficient matrices of equations (B-3) and (B-4) respectively. The values of $Q(0)$, $\delta^2 D^2 Q(0)$, $\delta^4 D^4 Q(0)$, $\delta^5 D^5 Q(0)$ and $\delta^6 D^6 Q(0)$ may be solved for by

$$\begin{bmatrix} Q(0) \\ \delta^2 D^2 Q(0) \\ \delta^4 D^4 Q(0) \\ \delta^5 D^5 Q(0) \\ \delta^6 D^6 Q(0) \end{bmatrix} = [A]^{-1} \begin{bmatrix} Q_1 \\ Q_2 \\ Q_3 \\ Q_4 \\ Q_5 \end{bmatrix} + O\delta^7 \quad (B-5)$$

Putting equation (B-5) into equation (B-4),

$$\begin{bmatrix} Q(\delta) \\ \delta DQ(\delta) \\ \delta^2 D^2 Q(\delta) \\ \delta^3 D^3 Q(\delta) \\ \delta^4 D^4 Q(\delta) \end{bmatrix} = [B][A]^{-1} \begin{bmatrix} Q_1 \\ Q_2 \\ Q_3 \\ Q_4 \\ Q_5 \end{bmatrix} + O\delta^7 \quad (B-6)$$

The last line of this set of equations gives

$$\begin{aligned} D^4 Q(\delta) = \frac{1}{\delta^4} & (-.911564626Q_1 + 2.750242955Q_2 - 3.043731779Q_3 \\ & + 1.42468416Q_4 - .219630709Q_5) + O\delta^3 \end{aligned} \quad (B-7)$$

To solve for $D^3 Q(\delta)$, the rightmost column and bottom row are eliminated from matrices [A] and [B] then these new matrices are inserted into equations (B-5) and (B-6).

The bottom line of equation (B-6) will now give the expression for $D^3Q(\delta)$ with a consistent third order truncation error. $D^2Q(\delta)$ and $DQ(\delta)$ were solved for in a similar manner.

$$D^3Q(\delta) = \frac{1}{\delta^3}(1.825165563Q_1 - 3.250331126Q_2 + 1.660927152Q_3 - .235761589Q_4) + O\delta^3 \quad (B-8)$$

$$D^2Q = \frac{1}{\delta^2}(-\frac{35}{60}Q_1 + \frac{8}{15}Q_2 + \frac{1}{20}Q_3) + O\delta^3 \quad (B-9)$$

$$DQ = \frac{1}{\delta}(-\frac{2}{3}Q_1 + \frac{2}{3}Q_2) + O\delta^3 \quad (B-10)$$

Due to the complexity of the boundary conditions, it was decided that consistent third order truncation error equations should also be used at $r = 2\delta$. For this the [B] matrix only need be changed as equation (B-2) is unchanged at this station. The new matrix [B] is formed by differentiating equation (B-2) and making the substitution $r = 2\delta$. Proceeding as for $r = \delta$ gives the following finite difference approximations

$$D^4Q(2\delta) = \frac{1}{\delta^4}(-3.10340136Q_1 + 6.903012634Q_2 - 5.342274053Q_3 + 1.66083577Q_4 - 0.123420797Q_5) + O\delta^3 \quad (B-11)$$

$$D^3Q(2\delta) = \frac{1}{\delta^3}(.868874172Q_1 - .937748345Q_2 - .254304636Q_3 + .323178808Q_4) + O\delta^3 \quad (B-12)$$

$$D^2Q(2\delta) = \frac{1}{\delta^2} \left(\frac{11}{12}Q_1 - \frac{28}{15}Q_2 + \frac{19}{20}Q_3 \right) + O\delta^3 \quad (B-13)$$

$$DQ(2\delta) = \frac{1}{\delta} \left(-\frac{4}{3}Q_1 + \frac{4}{3}Q_2 \right) + O\delta^3 \quad (B-14)$$

It should also be noted that the value of Q at $r = 0$ may be solved for from the top line of equations (B-5)

$$Q(0) = (1.795918367Q_1 - 1.24781341Q_2 + .606413994Q_3 - .177842566Q_4 + .023323615Q_5) + O\delta^3 \quad (B-15)$$

The central difference equations given by Ref. 6 were already consistent second order truncation error equations as confirmed by Ref. 8 and were retained.

For the wall, the clamped end, consistent second order equations (5) through (8) of Table II, Ref. 8 were modified for the "right boundary" using the procedure given in Section 5 of that reference.

$$D^4Q(1-\delta) = \frac{1}{\delta^4} \left(-\frac{1}{4}Q_{N-3} + \frac{8}{3}Q_{N-2} - 9Q_{N-1} + 16Q_N \right) + O\delta^2 \quad (B-16)$$

$$D^3Q(1-\delta) = \frac{1}{\delta^3} \left(-\frac{1}{3}Q_{N-2} + 3Q_N \right) + O\delta^2 \quad (B-17)$$

$$D^2Q(1-\delta) = \frac{1}{\delta^2} (Q_{N-1} - 2Q_N) + O\delta^2 \quad (B-18)$$

$$DQ(1-\delta) = \frac{1}{\delta} \left(-\frac{1}{2}Q_{N-1} \right) + O\delta^2 \quad (B-19)$$

Since the wall finite difference approximations were of only second order truncation error, the approximations for DQ through D^4Q at $r = 1-2\delta$ were obtained directly from the central difference equations with $Q(1) = 0$.

$$D^4Q(1-2\delta) = \frac{1}{\delta^4}(Q_{N-3} - 4Q_{N-2} + 6Q_{N-1} - 4Q_N) + O\delta^2 \quad (B-20)$$

$$D^3Q(1-2\delta) = \frac{1}{\delta^3}(-\frac{1}{2}Q_{N-3} + Q_{N-2} - Q_N) + O\delta^2 \quad (B-21)$$

$$D^2Q(1-2\delta) = \frac{1}{\delta^2}(Q_{N-2} - 2Q_{N-1} + Q_N) + O\delta^2 \quad (B-22)$$

$$DQ(1-2\delta) = \frac{1}{\delta}(-\frac{1}{2}Q_{N-2} + \frac{1}{2}Q_N) + O\delta^2 \quad (B-23)$$

APPENDIX C

NONUNIFORM MESH

To control the distribution of a fixed number of mesh points, a change of the independent variable from r to η was performed.

$$Q = Q(\eta) \quad (C-1)$$

$$r = r(\eta) \quad (C-2)$$

The derivative with respect to r becomes

$$D = (D^* r)^{-1} D^* \quad (C-3)$$

where

$$D^* = \frac{d}{d\eta} \quad \text{and} \quad D = \frac{d}{dr} \quad (C-4)$$

$DQ, D^2Q \dots$ can now be expressed in terms of the new independent variable, η .

$$DQ = (D^* r)^{-1} D^* Q \quad (C-5)$$

$$\begin{aligned} D^2Q &= D(DQ) = (D^* r)^{-1} D^* (DQ) \\ &= (D^* r)^{-2} D^{*2} Q - (D^* r)^{-3} (D^{*2} r) D^* Q \end{aligned} \quad (C-6)$$

$$\begin{aligned}
D^3 Q &= D(D^2 Q) = (D^* R)^{-1} D^* (D^2 Q) \\
&= (D^* r)^{-3} D^{*3} Q - 3(D^* r)^{-4} (D^{*2} r) D^{*2} Q \\
&\quad - [(D^* r)^{-4} (D^{*3} r) - 3(D^* r)^{-5} (D^{*2} r)^2] DQ \quad (C-7)
\end{aligned}$$

$$\begin{aligned}
D^4 Q &= D(D^3 Q) = (D^* r)^{-1} D^* (D^3 Q) \\
&= (D^* r)^{-4} D^{*4} Q - 6(D^* r)^{-5} (D^{*2} r) D^{*3} Q \\
&\quad + [15(D^* r)^{-6} (D^{*2} r) - 4(D^* r)^{-5} (D^{*3} r)] D^{*2} Q \\
&\quad - [15(D^* r)^{-7} (D^{*2} r)^3 - 10(D^* r)^{-6} (D^{*2} r) (D^{*3} r) \\
&\quad + (D^* r)^{-5} (D^{*4} r)] DQ \quad (C-8)
\end{aligned}$$

The derivatives of Q with respect to r can now be written

$$DQ = f_{11} D^* Q \quad (C-9)$$

$$D^2 Q = f_{22} D^{*2} Q + f_{21} D^* Q \quad (C-10)$$

$$D^3 Q = f_{33} D^{*3} Q + f_{32} D^{*2} Q + f_{31} D^* Q \quad (C-11)$$

$$D^4 Q = f_{44} D^{*4} Q + f_{43} D^{*3} Q + f_{42} D^{*2} Q + f_{41} D^* Q \quad (C-12)$$

where

$$f_{11} = (D^* r)^{-1} \quad (C-13)$$

$$f_{22} = (D^* r)^{-2} \quad (C-14)$$

$$f_{21} = -(D^* r)^{-3} (D^{*2} r) \quad (C-15)$$

$$f_{33} = (D^* r)^{-3} \quad (C-16)$$

$$f_{32} = -3 (D^* r)^{-4} (D^{*2} r) \quad (C-17)$$

$$f_{31} = 3 (D^* r)^{-5} (D^{*2} r)^2 - (D^* r)^{-4} (D^{*3} r) \quad (C-18)$$

$$f_{44} = (D^* r)^{-4} \quad (C-19)$$

$$f_{43} = -6 (D^* r)^{-5} (D^{*2} r) \quad (C-20)$$

$$f_{42} = 15 (D^* r)^{-6} (D^{*2} r)^2 - 4 (D^* r)^{-5} (D^{*3} r) \quad (C-21)$$

$$f_{41} = -15 (D^* r)^{-7} (D^{*2} r)^3 + 10 (D^* r)^{-6} (D^{*2} r) (D^{*3} r) \\ - (D^* r)^{-5} (D^{*4} r) \quad (C-22)$$

Substituting equations (C-9) through (C-12) into the vorticity transport equation (A-6) yields

$$M_4^* D^{*4} Q + M_3^* D^{*3} Q + M_2^* D^{*2} Q + M_1^* D^* Q + M_0^* Q \\ - \gamma [N_2^* D^{*2} Q + N_1^* D^* Q + N_0^* Q] = 0 \quad (C-23)$$

where

$$M_4^* = M_4 f_{44} \quad (C-24)$$

$$M_3^* = M_4 f_{43} + M_3 f_{33} \quad (C-25)$$

$$M_2^* = M_4 f_{42} + M_3 f_{32} + M_2 f_{22} \quad (C-26)$$

$$M_1^* = M_4 f_{41} + M_3 f_{31} + M_2 f_{21} \quad (C-27)$$

$$M_0^* = M_0 \quad (C-28)$$

$$N_2^* = N_2 f_{22} \quad (C-29)$$

$$N_1^* = N_2 f_{21} + N_1 f_{11} \quad (C-30)$$

$$N_0^* = N \quad (C-31)$$

In order to concentrate the mesh points at the axis, the function

$$r = 1 - C \tanh \lambda(1-\eta) \quad (C-32)$$

was chosen where λ is a parameter controlling the degree of concentration of mesh points near the axis. Equation (C-32) must satisfy the two conditions

$$r = 0 \quad \text{at} \quad \eta = 0 \quad (C-33)$$

and

$$r = 1 \quad \text{at} \quad \eta = 1 .$$

Substituting equation (C-33) into (C-32) gives

$$C = 1/\tanh \lambda . \quad (C-35)$$

Computing derivatives

$$D^* r = C\lambda / \cosh^2 \lambda (1-\eta) \quad (C-36)$$

$$D^{*2} r = 2C\lambda^2 [\tanh \lambda (1-\eta) / \cosh^2 \lambda (1-\eta)] \quad (C-37)$$

$$D^{*3} r = -2C\lambda^3 \{ [1-2\sinh^2 \lambda (1-\eta)] / \cosh^4 \lambda (1-\eta) \} \quad (C-38)$$

$$D^{*4} r = 8C\lambda^4 [\tanh^3 \lambda (1-\eta) / \cosh^2 \lambda (1-\eta)] \quad (C-39)$$

To shift the mesh point concentration to the wall, the function

$$r = C \tanh \lambda \eta \quad (C-40)$$

was selected. Satisfying equations (C-33) and (C-34) for this equation also gives equation (C-35). The derivatives

of (C-40) are given by equations (C-36) through (C-39) if η is substituted for all occurrences of $(1-\eta)$ and the signs of equations (C-37) and (C-39) are reversed. Figures C-1 and C-2 show equations (C-32) and (C-40) for four selected values of the parameter λ .

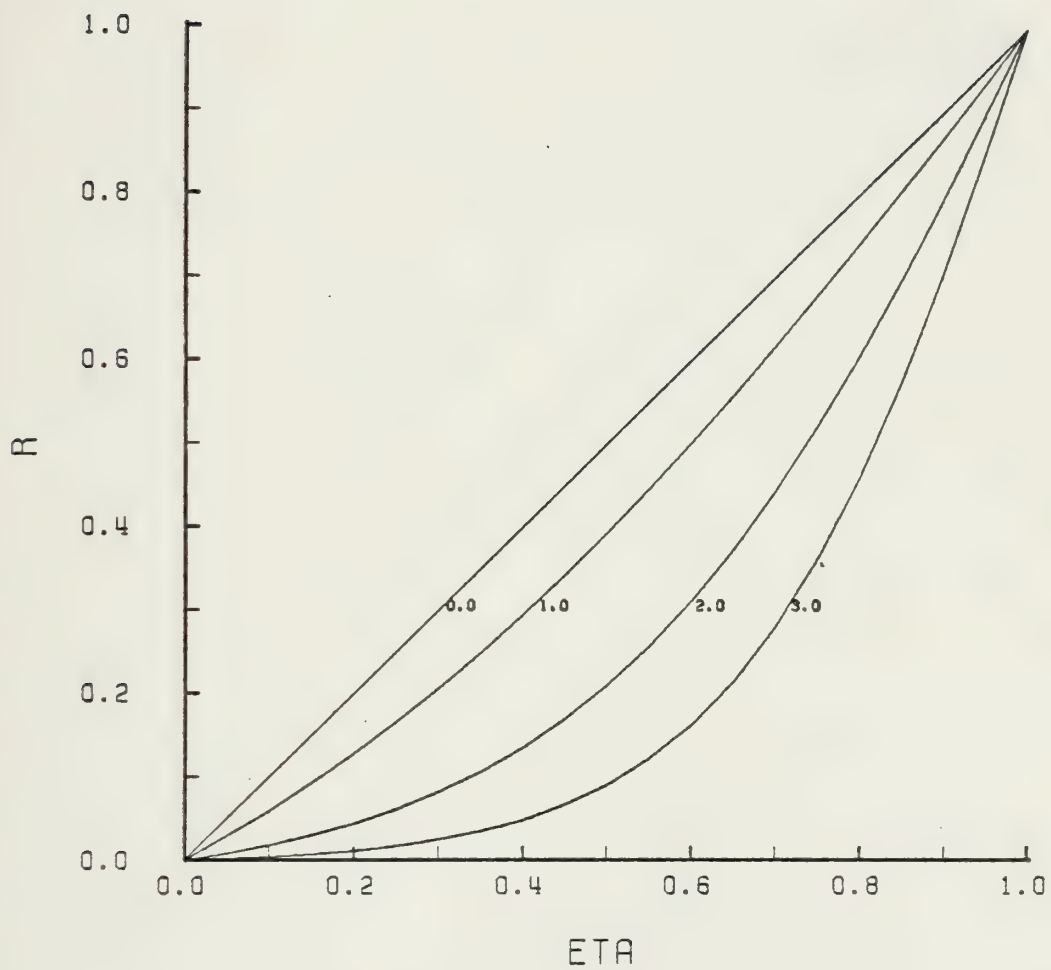


FIGURE C-1. R Versus η for Four Selected Values of Lambda - Axis Offset

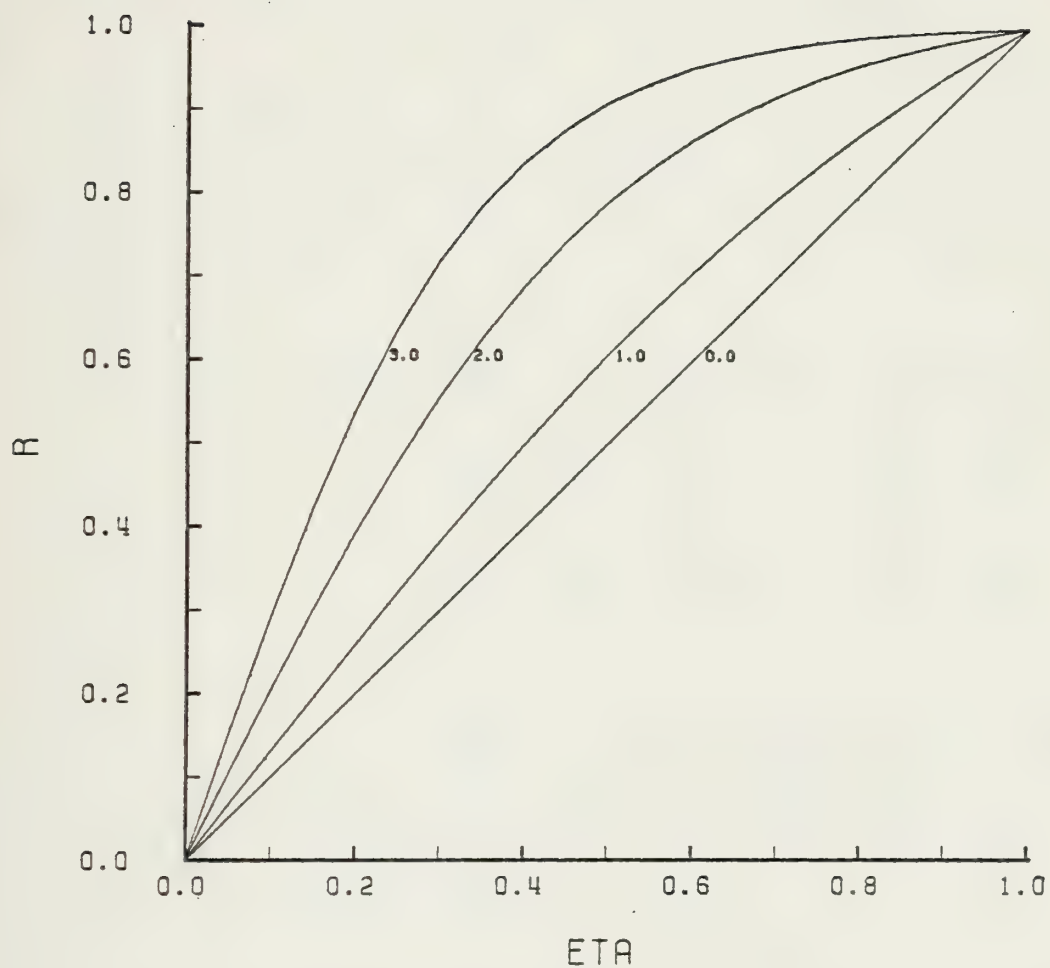


FIGURE C-2. R Versus η for Four Selected Values of λ - Wall Offset

APPENDIX D

DERIVATION OF PERTURBATION VELOCITIES

From Ref. 4, Appendix E, equations E-6 through E-8:

$$\begin{Bmatrix} u(r) \\ v(r) \\ w(r) \end{Bmatrix} = [A]\bar{W} + [B]D\bar{W} \quad (D-1)$$

$$= \begin{bmatrix} 0 & -\frac{\beta}{r} & \frac{1}{r} \\ \frac{\beta}{r} & 0 & -\alpha \\ 0 & \alpha & 0 \end{bmatrix} \begin{Bmatrix} F \\ G \\ H \end{Bmatrix} + \begin{bmatrix} 0 & 0 & 1 \\ 0 & 0 & 0 \\ -1 & 0 & 0 \end{bmatrix} \begin{Bmatrix} DF \\ DG \\ DG \end{Bmatrix} \quad (D-2)$$

For this case $\beta = \eta_i = 0$ and $F = DF = 0$. Restricting the investigation to the function H for the reason expressed in Section I and solving for $u(r)$ gives

$$u(r) = \frac{H}{r} + DH \quad (D-3)$$

Performing the change of variable

$$H = rQ \quad (D-4)$$

$$DH = Q + rDQ \quad (D-5)$$

$$u(r) = \frac{rQ}{r} + (Q + rDQ) = 2Q + rDQ \quad (D-6)$$

In order to implement this derivation in a numerical analysis, equation (D-6) was rewritten as

$$u_i = 2Q_i + r_i DQ_i \quad (D-7)$$

Performing the change of independent variable (Appendix C) to accommodate a nonuniform mesh

$$Q_i = Q(\eta_i) \quad (D-8)$$

$$r_i = r(\eta_i) \quad (D-9)$$

$$DQ_i = (D^* r_i)^{-1} D^* Q(\eta_i) \quad (D-10)$$

Substituting equations (D-8), (D-9) and (D-10) into equation (D-7) gives

$$u_i = 2Q(\eta_i) + r(\eta_i) D^* r_i^{-1} D^* Q(\eta_i) \quad (D-11)$$

For the axis offset nonuniform mesh, $r(\eta)$ is given by equation (C-32) and $(D^* r)$ by equation (C-36). Substituting into equation (D-11) using equation (C-35) results in

$$\begin{aligned}
u_i &= 2Q(\eta_i) + \left\{ 1 - \frac{\tanh[\lambda(1-\eta_i)]}{\tanh \lambda} \right\} \left\{ \frac{\cosh^2[\lambda(1-\eta_i)]}{C\lambda} \right\} D^* Q(\eta_i) \\
&= 2Q(\eta_i) + \left\{ 1 - \frac{\tanh[\lambda(1-\eta_i)]}{\tanh \lambda} \right\} \frac{\tanh \lambda \cosh^2[\lambda(1-\eta_i)]}{\lambda} \left\{ D^* Q(\eta_i) \right\} \\
&\hspace{25em} (D-12)
\end{aligned}$$

For the wall offset mesh, equation (C-40) is substituted for equation (C-32) and all occurrences of the term $1-\eta_i$ are replaced by the term η_i .

The value of u at the axis (u_0) and at the wall (u_{N+1}) were solved for by using the boundary conditions specified in Ref. 9, namely

$$Q(1) = 0 \hspace{15em} (D-13)$$

$$DQ(1) = 0 \hspace{15em} (D-14)$$

$$DQ(0) = 0 \hspace{15em} (D-15)$$

$$D^3Q(0) = 0 \hspace{15em} (D-16)$$

From equations (D-13) and (D-14), using equation (D-7) it is obvious that

$$u_{N+1} = 0 \hspace{15em} (D-17)$$

and from equations (D-15) and (D-7), it is similarly found that

$$u_0 = 2Q(0) , \quad (D-18)$$

where the finite difference approximation for $Q(0)$ is given by equation (B-15).


```

10.....
20PROGRAM PIPEO (CP/CMS VERSION)
30
40PROGRAM TO INVESTIGATE FLOW STABILITY AND CHARACTERISTICS
50FOR THE 3-D CYLINDRICAL FLOW PROBLEM
60NI=0; FOR THE FUNCTION Q
70
80TO OBTAIN A FLOW CHART OF THIS PROGRAM, CONSULT NAVAL
90POSTGRADUATE SCHOOL TECHNICAL NOTE TN 0141-25, "USER'S
100GUIDE TO THE PROGRAMMING AIDS LIBRARY", UNDER PROGRAM
110FLOWCH.
120
130
140
150
160-----
170IMPLICIT REAL*8(A-H,O-Z)
180DIMENSION AIPLT(20), REYPLT(20)
190COMPLEX *16A,G
200INTEGER *4CLOCK(6)
210COMMON /COEFNT/ A,G,REY,DELR,AMDA
220-----
230
240INPUT DESIRED MODE NUMBER
250
260
270
280WRITE (6,6) MODENO
290READ (5,7) MODENO
300CALL IXCLOCK (CLOCK)
310WRITE (6,8) CLOCK(3),CLOCK(4)
320IF (MODENO.EQ.2) GO TO 2
330
340*****
350CALCULATE STABILITY AT A POINT (MODENO = 1 & 3)
360
370
380
390
400
410
420
430
440
450
460
470
480

```

OUTPUTS DATA TO FILE FT02F001 COMPATIBLE WITH PROGRAM EIGFCN &
 PRINTS THE VALUE OF THE LEAST STABLE EIGENVALUE(GAMMA*) AT THE
 CONSOLE FOR EACH SET OF INPUT CONDITIONS. DATA IS ENTERED IN
 *D, FORMAT WITH A ZERO EXPONENT (I.E., 1.D0, 150.D0, -500, ETC.).
 RUN IS TERMINATED WHEN A NEGATIVE VALUE FOR REYNOLDS NUMBER IS
 ENTERED. THE TYPE OF MESH OFFSET IS DETERMINED BY THE VALUE
 OF LAMBDA. IF LAMBDA < -1.D-10, KSET IS SET EQUAL TO -1; IF
 LAMBDA > 1.D-10, KSET IS SET EQUAL TO 1; OTHERWISE KSET = 0.
 IF MODENO = 1, THE EIGENVECTOR CORRESPONDING TO THE LEAST
 STABLE EIGENVALUE (GAMMA*) WILL BE WRITTEN TO FILE FT02F001.


```

C      IF MODENO = 3, THIS OUTPUT IS INHIBITED.  MODENO MUST BE
C      SET EQUAL TO ONE TO GENERATE CORRECT DATA FOR PROGRAM EIGFCN.
C      *****
C      1  WRITE (6,9)  AMDA
C          READ (5,11)  AMDA
C          KSET = 0
C          IF (AMDA.LT.-1.D-10) KSET=-1
C          IF (AMDA.GT.1.D-10) KSET=1
C          WRITE (6,10)
C          READ (5,11)  AR
C          WRITE (6,12)
C          READ (5,11)  AI
C          WRITE (6,13)
C          READ (5,11)  REY
C          IF (REY.LE.0.D0) GO TO 5
C          CALL STAB (AR, AI, GRMAX, KSET, MODENO)
C          WRITE (6,14)  GRMAX
C          GO TO 1
C      *****
C      COMPUTE STABILITY MAP (MODENO = 2)
C
C      COMPUTES A STABILITY MAP AT MESH POINTS ESTABLISHED BY
C      THE FOLLOWING PARAMETERS READ FROM FILE FTOLF001:
C
C      NXSTP - NO OF MESH PTS IN X-DIRECTION
C      NYSTP - NO OF MESH PTS IN Y-DIRECTION
C      N - DIMENSION OF MATRICES X & Y IN SUBROUTINE STAB
C      DELAR - MAGNITUDE OF THE X-DIRECTION STEP
C      DELAI - MAGNITUDE OF THE Y-DIRECTION STEP
C      REY - REYNOLDS NUMBER
C
C      **NOTE - RUN TIME IS LONG IN THIS MODE, SO CP/CMS
C      RUNS SHOULD BE LIMITED TO 10X10 MESHES, OR LESS WITH
C      N = 31.  LARGER RUNS SHOULD BE MADE UNDER BATCH.
C      LITTLE OS MAY ALSO BE USED AS LESS THAN 180K OF
C      CORE IS REQUIRED IN THIS MODE FOR N <= 47.
C
C      **NOTE - TO RUN THE MAPPING PORTION UNDER OS OR LITTLE OS,
C      PERFORM THE FOLLOWING:
C
C      1) RETAIN ALL MAIN PROGRAM SECTIONS BRACKETED BY '-----'.
C      2) CHANGE ALL READ DEVICES TO '5'. VICE '1' IN MAIN PROGRAM.
C      3) CHANGE THE DEVICE CODE OF THE LAST WRITE STATEMENT

```



```

290
300
310
320
330
340
350
360
370
380
390
400
410
420
430
440
450
460
470
480
490
500
510
520
530
540
550
560
570
580
590
600
610
620
630
640
650
660
670
680
690
700
710
720
730
740
750
760

```

MODENO - AN INTEGER CONTROLLING THE OUTPUT OF
OF EIGENVECTORS TO FILE FT02FO01. IF MODENO
IS EQUAL TO +1, EIGENVECTORS ARE OUTPUT;
OTHERWISE OUTPUT IS INHIBITED.

OTHER ROUTINES NEEDED

MSET2,CDMTIN,MULM,DSPLIT,EHESSC,ELRH2C,EBALAC,EBBCKC

.....

SUBROUTINE STAB (AR,AI,GRMAX,KSET,MODENO)
IMPLICIT REAL*8 (A-H,O-Z)
COMPLEX *16A,G
COMPLEX *16CQM1E1,CQM2E1

NOTE--CHANGE DIMENSIONS FROM HERE THROUGH 'N' = ' FOR
NEW NMESH. Cp/CMS MAX NMESH IS 79. LOGIN WITH 520K OF CORE.

REAL *8GR(79),GI(79),ZR(79,79),ZI(79,79),RADIUS(79),DVEC(79)
COMPLEX *16XMAT(79,79),YMAT(79,79),WV(79)
DIMENSION IVEC(79)
COMMON /COEFNT/ A,G,REY,DELR,AMDA
EXTERNAL CQM1E1,CQM2E1

A = DCMLPX(AR,AI)
MDIM = 79
N = 79

SET UP THE CENTRAL DIFFERENCE APPROXIMATION AT EACH POINT IN
THE MESH FOR THOSE TERMS IN THE VORTICITY TRANSPORT EQUATION
WHICH DO NOT CONTAIN GAMMA AS A FACTOR.

CALL MSET2 (XMAT,N,MDIM,CQM1E1,KSET)

SET UP THE CENTRAL DIFFERENCE APPROXIMATION AT EACH POINT IN
THE MESH FOR THOSE TERMS IN THE VORTICITY TRANSPORT EQUATION
WHICH CONTAIN GAMMA AS A FACTOR.

CALL MSET2 (YMAT,N,MDIM,CQM2E1,KSET)

DZL

NON

[illegible]


```

100 CALL MSET2(X,N,MDIM,CFMAT,KSET)
110
120 DESCRIPTION OF PARAMETERS
130
140 X - THE NAME OF THE ARRAY BEING GENERATED. MUST BE DIMENSIONED
150 IN THE CALLING PROGRAM
160
170 N- THE ROW DIMENSION OF THE MATRIX X. MUST BE .GE. N.
180
190 MDIM - THE COLUMN DIMENSION OF THE MATRIX X. MUST BE .GE. N.
200
210 CFMAT - THE NAME OF A FUNCTION SUBPROGRAM WITH 4 PARAMETERS,
220 JSTA, K, CQM1 & CQM2. CFMAT MUST BE DECLARED
230 EXTERNAL IN THE CALLING PROGRAM.
240
250 THE FOLLOWING IS OUTPUT BY MSET2
260
270 X - THE N BY N MATRIX INTO WHICH THE COEFFICIENTS OF THE CENTRAL
280 DIFFERENCING ARE PUT.
290
300 OTHER ROUTINES NEEDED
310
320 FUNCTION SUBPROGRAM NAME PASSED IN THE CALLING PARAMETER 'CFMAT'
330 AND MSET1.
340 .....
350
360 SUBROUTINE MSET2 (X,N,MDIM,CFMAT,KSET)
370 REAL *8REY,R,DEL,DFLOAT,AMDA,ETA
380 COMPLEX *16X(MDIM,MDIM),CQM1(5),CQM2(3)
390 COMPLEX *16A,G
400 COMPLEX *16CFMAT
410 COMMON /COEFNT/ A,G,REY,DEL,AMDA
420
430 DEFINE THE SPACING OF THE INTERIOR MESH POINTS.
440
450 DEL = 1D0/DFLOAT(N+1)
460
470
480 INITIALIZE ALL ELEMENTS IN THE ARRAY TO ZERO.
490
500
510 DO 1 I=1,N
520 DO 1 J=1,N
530
540
550
560
570

```


RETURN
END

MST21060
MST21070

.....FUNCTION CQM1E1(JSTA,K,CQM1,CQM2).....
(POLAR COORDINATES)

CQM1 10
CQM1 20
CQM1 30
CQM1 40
CQM1 50
CQM1 60
CQM1 70
CQM1 80
CQM1 90
CQM1 100
CQM1 110
CQM1 120
CQM1 130
CQM1 140
CQM1 150
CQM1 160
CQM1 170
CQM1 180
CQM1 190
CQM1 200
CQM1 210
CQM1 220
CQM1 230
CQM1 240
CQM1 250
CQM1 260
CQM1 270
CQM1 280
CQM1 290
CQM1 300
CQM1 310
CQM1 320
CQM1 330
CQM1 340
CQM1 350
CQM1 360
CQM1 370
CQM1 380
CQM1 390
CQM1 400
CQM1 410
CQM1 420
CQM1 430
CQM1 440

PURPOSE

RETURNS THE VALUES FOR THE COEFFICIENTS IN THE ARRAYS
REPRESENTING THE CENTRAL DIFFERENCE APPROXIMATION OF THE
VORTICITY TRANSPORT EQUATION USING THE COEFFICIENTS COMPUTED
BY SUBROUTINE MSET1.

DESCRIPTION OF PARAMETERS

JSTA - INDICATES WHICH DIFFERENCE EQUATION SET WILL BE USED.

- JSTA=1 - CONSISTENT 3RD ORDER TRUNCATION ERROR FINITE
DIFFERENCE EQUATIONS FOR R=DEL WILL BE USED.
- JSTA=2 - SAME AS ABOVE BUT R=2DO*DEL
- JSTA=3 - CENTRAL DIFFERENCE EQUATIONS WITH CONSISTENT 2ND
ORDER TRUNCATION ERROR WILL BE USED.
- JSTA=4 - SAME AS JSTA=3 BUT FOR R=1DO-2DO*DEL.
- JSTA=5 - SAME AS ABOVE BUT FOR R=1DO-DEL.

K - INDICATES THE ABSOLUTE POSITION OF THE POINT IN EACH ROW
OF THE FINITE DIFFERENCE MESH. IF THE FIRST NON-ZERO ENTRY
IN ROW J IS ELEMENT(J,3), THEN K=1 DENOTES ELEMENT(J,3),
K=2 DENOTES ELEMENT(J,4), ETC.

CQM1,CQM2 - THE COEFFICIENT ARRAYS FOR THE FINITE DIFFERENCE
APPROXIMATION OF THE FUNCTION Q. CQM1 CONTAINS THE
COEFFICIENTS FOR THE NON-GAMMA TERMS, WHILE CQM2 CONTAINS
THE COEFFICIENTS OF THE GAMMA TERMS. BOTH ARRAYS MUST BE
DIMENSIONED COMPLEX*16.

EXAMPLE OF THE CALLING ARGUMENT:

CQ M(1,2) E1(JSTA,K,CQM1,CQM2)

CQ - Q COMPONENT OF THE VELOCITY VECTOR POTENTIAL.

M(1,2) - 1 REFERS TO TERMS NOT CONTAINING GAMMA AS A
FACTOR.

2 REFERS TO TERMS CONTAINING GAMMA AS A FACTOR.


```

123D0*CQM1(3)/(15D0*DEL**2)+4D0*CQM1(2)/(3D0*DEL)+CQM1(1)
GO TO 29
10 CQM1E1 = -5.342274053D0*CQM1(5)/DEL**4-.254304636D0*CQM1(4)/DEL**3
1+19D0*CQM1(3)/(20D0*DEL**2)
GO TO 29
11 CQM1E1 = 1.666083577D0*CQM1(5)/DEL**4+.3231788C8D0*C*CQM1(4)/DEL**3
GO TO 29
12 CQM1E1 = -0.123420797D0*CQM1(5)/DEL**4
GO TO 29

      CENTRAL DIFFERENCE APPROXIMATION FOR COMPONENT Q (NON GAMMA).

13 GO TO (14,15,16,17,18),K
14 CQM1E1 = CQM1(5)/DEL**4-CQM1(4)/(2D0*DEL**3)
GO TO 29
15 CQM1E1 = -4D0*CQM1(5)/DEL**4+CQM1(4)/DEL**3+CQM1(3)/DEL**2-CQM1(2)
1/(2D0*DEL)
GO TO 29
16 CQM1E1 = 6D0*CQM1(5)/DEL**4-2D0*CQM1(3)/DEL**2+CQM1(1)
GO TO 29
17 CQM1E1 = -4D0*CQM1(5)/DEL**4-CQM1(4)/DEL**3+CQM1(3)/DEL**2+CQM1(2)
1/(2D0*DEL)
GO TO 29
18 CQM1E1 = CQM1(5)/DEL**4+CQM1(4)/(2D0*DEL**3)
GO TO 29

      FINITE DIFFERENCE EQUATIONS AT ETA=1D0-2D0*DEL (NCN-GAMMA).

19 GO TO (20,21,22,23),K
20 CQM1E1 = CQM1(5)/DEL**4-0.5D0*CQM1(4)/DEL**3
GO TO 29
21 CQM1E1 = -4D0*CQM1(5)/DEL**4+CQM1(4)/DEL**3+CQM1(3)/DEL**2-CQM1(2)
1/(2D0*DEL)
GO TO 29
22 CQM1E1 = 6D0*CQM1(5)/DEL**4-2D0*CQM1(3)/DEL**2+CQM1(1)
GO TO 29
23 CQM1E1 = -4D0*CQM1(5)/DEL**4-CQM1(4)/DEL**3+CQM1(3)/DEL**2+CQM1(2)
1/(2D0*DEL)
GO TO 29

      FINITE DIFFERENCE EQUATIONS AT ETA=1D0-DEL (NON GAMMA).

24 GO TO (25,26,27,28),K
25 CQM1E1 = -0.25D0*CQM1(5)/DEL**4
GO TO 29
26 CQM1E1 = 8D0*CQM1(5)/(3D0*DEL**4)-CQM1(4)/(3D0*DEL**3)
GO TO 29
27 CQM1E1 = -9D0*CQM1(5)/DEL**4+CQM1(3)/DEL**2-CQM1(2)/(2D0*DEL)
GO TO 29

```

C
C
C

C
C
C

C
C
C


```

GO TO 29
28 CQM1E1 = 16D0*CQM1(5)/DEL**4+3D0*CQM1(4)/DEL**3-2D0*CQM1(3)/DEL**2
1+CQM1(1)
25 RETURN
C
ENTRY CQM2E1(JSTA,K,CQM1,CQM2)
C
GO TO (30,35,40,45,50), JSTA
C
FINITE DIFFERENCE EQUATIONS AT ETA=DEL ( GAMMA ).
C
30 GO TO (31,32,33,34,35), K
31 CQM2E1 = -35D0*CQM2(3)/(60D0*DEL**2)-2D0*CQM2(2)/(3D0*DEL)+CQM2(1)
GO TO 54
32 CQM2E1 = 8D0*CQM2(3)/(15D0*DEL**2)+2D0*CQM2(2)/(3D0*DEL)
GO TO 54
33 CQM2E1 = CQM2(3)/(20D0*DEL**2)
GO TO 54
34 CQM2E1 = (0D0,0D0)
GO TO 54
C
FINITE DIFFERENCE EQUATIONS AT ETA=2D0*DEL ( GAMMA )
C
35 GO TO (36,37,38,39,40), K
36 CQM2E1 = 11D0*CQM2(3)/(12D0*DEL**2)-4D0*CQM2(2)/(3D0*DEL)
GO TO 54
37 CQM2E1 = -28D0*CQM2(3)/(15D0*DEL**2)+4D0*CQM2(2)/(3D0*DEL)+CQM2(1)
GO TO 54
38 CQM2E1 = 19D0*CQM2(3)/(20D0*DEL**2)
GO TO 54
39 CQM2E1 = (0D0,0D0)
GO TO 54
C
CENTRAL DIFFERENCE EQUATIONS FOR THE COMPONENT Q ( GAMMA ).
C
40 GO TO (41,42,43,44,45), K
41 CQM2E1 = (0D0,0D0)
GO TO 54
42 CQM2E1 = CQM2(3)/DEL**2-CQM2(2)/(2D0*DEL)
GO TO 54
43 CQM2E1 = -2D0*CQM2(3)/DEL**2+CQM2(1)
GO TO 54
44 CQM2E1 = CQM2(3)/DEL**2+CQM2(2)/(2D0*DEL)
GO TO 54
C
FINITE DIFFERENCE EQUATIONS AT ETA=1D0-2D0*DEL ( GAMMA ).
C
45 GO TO (46,47,48), K
46 CQM2E1 = CQM2(3)/DEL**2-CQM2(2)/(2D0*DEL)

```



```

GC TO 54      -2D0*CQM2(3)/DEL**2+CQM2(1)
47 CQM2E1 =
GC TO 54      CQM2(3)/DEL**2+CQM2(2)/(2D0*DEL)
48 CQM2E1 =
GC TO 54      (0D0,0D0)
49 CQM2E1 =
GC TO 54      (0D0,0D0)

      FINITE DIFFERENCE EQUATIONS AT ETA=1D0-DEL ( GAMMA ).

50 GO TO (53,51,52), K
51 CQM2E1 = CQM2(3)/DEL**2-CQM2(2)/(2D0*DEL)
GC TO 54
52 CQM2E1 = -2D0*CQM2(3)/DEL**2+CQM2(1)
GC TO 54      (0D0,0D0)
53 CQM2E1 =
54 RETURN
END

```

CQM11890
 CQM11900
 CQM11910
 CQM11920
 CQM11930
 CQM11940
 CQM11950
 CQM11960
 CQM11970
 CQM11980
 CQM11990
 CQM12000
 CQM12010
 CQM12020
 CQM12030
 CQM12040
 CQM12050
 CQM12060

```

..... SUBROUTINE CDMTIN(N,A,NDIM,IERR).....
PURPOSE
      INVERT A COMPLEX*16 MATRIX
USAGE
      CALL CDMTIN(N,A,NDIM,DETERM)
DESCRIPTION OF PARAMETERS
      N      - ORDER OF COMPLEX*16 MATRIX TO BE INVERTED
              (INTEGER) MAXIMUM 'N' IS 100
      A      - COMPLEX*16 INPUT MATRIX (DESTROYED). THE
              INVERSE OF 'A' IS RETURNED IN ITS PLACE
      NDIM   - THE SIZE TO WHICH 'A' IS DIMENSIONED
              (ROW DIMENSION OF 'A' ACTUALLY APPEARING
              IN THE DIMENSION STATEMENT OF USER'S
              CALLING PROGRAM)
      IERR   - ERROR PARAMETER RETURNED BY CDMTIN. IERR = 0 INDICATES
              NORMAL INVERSION. IERR = 9999 INDICATES SINGULAR MATRIX.
REMARKS

```

CDMT 10
 CDMT 20
 CDMT 30
 CDMT 40
 CDMT 50
 CDMT 60
 CDMT 70
 CDMT 80
 CDMT 90
 CDMT 100
 CDMT 110
 CDMT 120
 CDMT 130
 CDMT 140
 CDMT 150
 CDMT 160
 CDMT 170
 CDMT 180
 CDMT 190
 CDMT 200
 CDMT 210
 CDMT 220
 CDMT 230
 CDMT 240
 CDMT 250
 CDMT 260
 CDMT 270
 CDMT 280


```

ICOLU = K
AMAX = A(J,K)
6 CONTINUE
7 CCNTINUE
  IPIVOT(ICOLU) = IPIVOT(ICOLU)+1
  INTERCHANGE ROWS TO PUT PIVOT ELEMENT ON DIAGONAL
  IF (IROW-ICCLU) 8,10,8
8 CONTINUE
  DC 9 L=1,N
  SWAP = A(IROW,L)
  A(IROW,L) = A(ICOLU,L)
  9 A(ICOLU,L) = SWAP
  SWAP = ALPHA(IROW)
  ALPHA(IROW) = ALPHA(ICOLU)
  ALPHA(ICOLU) = SWAP
10 INDEX(I,1) = IROW
  INDEX(I,2) = ICOLU
  PIVOT(I) = A(ICOLU, ICOLU)
  U = PIVOT(I)
  TEMP = PIVOT(I)*DCONJG(PIVOT(I))
  IF (TEMP) 11,20,11
    DIVIDE PIVOT ROW BY PIVOT ELEMENT
11 A(ICOLU,ICOLU) = (1CO,0D0)
  DC 12 L=1,N
  U = PIVOT(I)
12 A(ICOLU,L) = A(ICOLU,L)/U
  REDUCE NON-PIVOT ROWS
13 IF (L1-1,N) 13,15,13
  T = A(L1,ICOLU)
  A(L1,ICOLU) = (0CO,0D0)
  DC 14 L=1,N
  U = A(ICOLU,L)
14 A(L1,L) = A(L1,L)-U*T

```


C	15	CONTINUE	CDMT11250
C			CDMT11260
C	16	CONTINUE	CDMT11270
C			CDMT11280
C		INTERCHANGE COLUMNS	CDMT11290
C			CDMT11300
C			CDMT11310
C			CDMT11320
C			CDMT11330
		DO 19 I=1,N	CDMT11340
		L = N+1-I	CDMT11350
		IF (INDEX(L,1)-INDEX(L,2)) 17,19,17	CDMT11360
	17	JROW = INDEX(L,1)	CDMT11370
		JCOLUMN = INDEX(L,2)	CDMT11380
C			CDMT11390
		DO 18 K=1,N	CDMT11400
		SWAP = A(K,JROW)	CDMT11410
		A(K,JROW) = A(K,JCOLUMN)	CDMT11420
		A(K,JCOLUMN) = SWAP	CDMT11430
	18	CONTINUE	CDMT11440
C			CDMT11450
C	19	CONTINUE	CDMT11460
			CDMT11470
		RETURN	CDMT11480
	20	WRITE (6,22)	CDMT11490
		IERR = 9999	CDMT11500
	21	RETURN	CDMT11510
C	22	FORMAT (20H MATRIX IS SINGULAR)	CDMT11520
		END	CDMT11530
C			CDMT11540
C	 SUBROUTINE MULM(X1,X2,N,MDIM,TEMPV).....	MULM 10
C		PURPOSE	MULM 20
C		PERFORMS THE MATRIX MULTIPLICATION OF A SQUARE MATRIX BY A	MULM 30
C		SQUARE MATRIX. THE RESULT IS RETURNED IN MATRIX X1.	MULM 40
C		USAGE	MULM 50
C			MULM 60
C			MULM 70
C			MULM 80
C			MULM 90
C		CALL MULM(X1,X2,N,MDIM,TEMPV)	MULM 100
C		DESCRIPTION OF PARAMETERS	MULM 110
C			MULM 120
C		X1 - THE MULTIPLYING MATRIX ON INPUT AND THE RESULTANT PRODUCT	MULM 130
C		ON OUTPUT.	MULM 140
C			MULM 150
C			MULM 160

[illegible][illegible]

.....SUBROUTINE DSPLIT(N,MDIM,A,AR,AI).....	DSPL	10
PURPOSE	DSPL	20
DSPLIT TAKES A MATRIX OF COMPLEX*16 NUMBERS AND	DSPL	30
SPLITS IT INTO TWO MATRICES, ONE CONTAINING THE REAL	DSPL	40
PART OF THE ORIGINAL MATRIX, AND ONE CONTAINING THE	DSPL	50
IMAGINARY PART.	DSPL	60
USAGE	DSPL	70
CALL DSPLIT(N,MDIM,A,AREAL,AIMAG)	DSPL	80
DESCRIPTION OF PARAMETERS	DSPL	90
N - THE SIZE OF THE MATRIX A, AN N BY N SQUARE	DSPL	100
MATRIX.	DSPL	110
MDIM - THE COLUMN DIMENSION OF MATRIX A	DSPL	120
A - THE INPUT MATRIX. MUST BE DIMENSIONED MDIM BY	DSPL	130
AT LEAST N IN THE CALLING PROGRAM (COMPLEX*16)	DSPL	140
AREAL,AIMAG - THE OUTPUT MATRICES CONTAINING THE	DSPL	150
REAL AND IMAGINARY PARTS, RESPECTIVELY, OF	DSPL	160
MATRIX A. MUST BE DIMENSIONED (MDIM,MDIM) IN THE	DSPL	170
CALLING PROGRAM.	DSPL	180
NOTES....	DSPL	190
MATRIX A AND MATRIX AREAL MAY OVERLAP IF THEY ARE	DSPL	200
DIMENSIONED IN THE CALLING PROGRAM AS FOLLOWS...	DSPL	210
COMPLEX*16 A(MDIM,MDIM)	DSPL	220
REAL*8 AREAL(MDIM,MDIM),AIMAG(MDIM,MDIM)	DSPL	230
EQUIVALENCE(A(1,1),AREAL(1,1))	DSPL	240
OTHER ROUTINES NEEDED	DSPL	250
NONE	DSPL	260
SUBROUTINE DSPLIT (N,MDIM,A,AR,AI)	DSPL	270
REAL *8A(2,MDIM,MDIM),AR(MDIM,MDIM),AI(MDIM,MDIM)	DSPL	280
	DSPL	290
	DSPL	300
	DSPL	310
	DSPL	320
	DSPL	330
	DSPL	340
	DSPL	350
	DSPL	360
	DSPL	370
	DSPL	380
	DSPL	390
	DSPL	400
	DSPL	410
	DSPL	420
	DSPL	430
	DSPL	440
	DSPL	450
	DSPL	460
	DSPL	470
	DSPL	480

DSPL 490
DSPL 500
DSPL 510
DSPL 520
DSPL 530
DSPL 540
DSPL 550
DSPL 560
DSPL 570
DSPL 580

```

C      DO 1 J=1,N
C      DO 1 I=1,N
C      AR(I,J) = A(1,I,J)
C      1 AI(I,J) = A(2,I,J)
C
C      RETURN
C      END

```

```

C      SUBROUTINE EBALAC (AR,AI,N,IA,K,L,D)
C-----D-----LIBRARY 1-----
C      FUNCTION
C      USAGE
C      PARAMETERS      AR
C                      AI
C
C      N
C      IA
C      K
C      L
C
C      D
C
C      PRECISION
C      LANGUAGE
C
C      LATEST REVISION      MARCH 9, 1977
C
C      SUBROUTINE EBALAC (AR,AI,N,IA,K,L,D)
C
C      DIMENSION
C                      AR(IA,1),AI(IA,1),D(N)

```

EBAC0010
EBAC0020
EBAC0030
EBAC0040
EBAC0050
EBAC0060
EBAC0070
EBAC0080
EBAC0090
EBAC0100
EBAC0110
EBAC0120
EBAC0130
EBAC0140
EBAC0150
EBAC0160
EBAC0170
EBAC0180
EBAC0190
EBAC0200
EBAC0210
EBAC0220
EBAC0230
EBAC0240
EBAC0250
EBAC0260
EBAC0270
EBAC0280
EBAC0290
EBAC0300
EBAC0310
EBAC0320
EBAC0330
EBAC0340
EBAC0350
EBAC0360

```

C      - BALANCES A COMPLEX GENERAL MATRIX AND ISOLATES
C      EIGENVALUES WHENEVER POSSIBLE.
C      - CALL EBALAC (AR,AI,N,IA,K,L,D)
C      - INPUT/OUTPUT MATRICES OF DIMENSION N BY N.
C      ON INPUT, AR AND AI CONTAIN THE REAL
C      AND IMAGINARY PARTS, RESPECTIVELY, OF
C      THE COMPLEX MATRIX OF ORDER N TO BE
C      BALANCED. ON OUTPUT, AR AND AI CONTAIN THE
C      REAL AND IMAGINARY PARTS OF THE
C      TRANSFORMED MATRIX.
C      - INPUT VARIABLE CONTAINING THE ORDER
C      OF THE MATRIX A = (AR,AI) TO BE BALANCED.
C      - INPUT VARIABLE CONTAINING THE ROW DIMENSION OF
C      AR AND AI IN THE CALLING PROGRAM.
C      - OUTPUT INTEGERS CONTAINING THE BOUNDARY
C      INDICES FOR THE BALANCED MATRIX A = (AR,AI)
C      SUCH THAT
C      AR(I,J) = 0. AND AI(I,J) = 0. IF
C      (1) I IS GREATER THAN J AND
C      (2) J = 1,...,K-1 OR
C      I = L+1,...,N
C      - OUTPUT VECTOR OF LENGTH N CONTAINING
C      INFORMATION DETERMINING THE PERMUTATIONS
C      USED AND THE SCALING FACTORS.
C      - SINGLE/DOUBLE
C      - FORTRAN

```



```

C      M = L
C      IEXC = 1
C      GO TO 5
40 CONTINUE
C      GO TO 50
C
C      45 K = K+1
C      50 DO 60 J = K,L
C          DO 55 I = K,L
C              IF (I.EQ.J) GC TO 55
C              IF (AR(I,J).NE.ZERO) .OR. AI(I,J).NE.ZERO) GO TO 60
C          CONTINUE
C      55 M = K
C      IEXC = 2
C      GO TO 5
C      60 CONTINUE
C
C      DO 65 I = K,L
C      D(I) = ONE
C      CONTINUE
C      65 NOCONV = .FALSE.
C      DO 110 I = K,L
C          C = ZERO
C          R = ZERO
C          DO 75 J = K,L
C              IF (J.EQ.I) GO TO 75
C              C = C+DABS(AR(J,I))+DABS(AI(J,I))
C              R = R+DABS(AR(I,J))+DABS(AI(I,J))
C          CONTINUE
C      75 G = R*RRADIX
C      F = ONE
C      S = C+R
C      80 IF (C.GE.G) GO TO 85
C      F = F*RADIX
C      C = C*B2
C      GO TO 80
C      85 G = R*RADIX
C      90 IF (C.LT.G) GO TO 95
C      F = F*RRADIX
C      C = C*RB2
C      GO TO 90
C      95 IF ((C+R)/F.GE.PT95*S) GO TO 110
C      G = ONE/F
C      D(I) = D(I)*F

```



```

NOCONV = .TRUE.
DO 100 J = K, N
  AR(I, J) = AR(I, J)*G
  AI(I, J) = AI(I, J)*G
100 CONTINUE
DO 105 J = 1, L
  AR(J, I) = AR(J, I)*F
  AI(J, I) = AI(J, I)*F
105 CONTINUE
110 CONTINUE
IF (NOCONV) GO TO 70
115 RETURN
END

```

SUBROUTINE EHESCC (AR, AI, K, L, N, IA, ID)

-----D-----LIBRARY 1-----

FUNCTION

USAGE
PARAMETERS AR

- REDUCTION OF A COMPLEX MATRIX TO COMPLEX
UPPER HESSENBERG FORM.
- CALL EHESCC(AR, AI, K, L, N, IA, ID)
- INPUT/OUTPUT MATRIX OF DIMENSION N BY N* OF
ON INPUT CONTAINS THE REAL COMPONENTS OF
THE MATRIX TO BE REDUCED.
ON OUTPUT CCNTAINS THE REAL COMPONENTS
OF THE REDUCED HESSENBERG FORM IN THE
UPPER TRIANGULAR PORTION (INCLUDING MAIN
AND SUB-DIAGONAL) AND THE DETAILS OF
THE REDUCTION IN THE LOWER TRIANGULAR
PORTION.
- INPUT/OUTPUT MATRIX OF DIMENSION N BY N
CONTAINING THE IMAGINARY COUNTERPARTS
TO AR, ABOVE.
- INPUT SCALAR CONTAINING THE ROW AND COLUMN
INDEX OF THE STARTING ELEMENT TO BE
REDUCED BY ROW SCALING. FOR UNBALANCED
MATRICES SET K = 1.
- INPUT SCALAR CONTAINING THE ROW AND
COLUMN INDEX OF THE LAST ELEMENT TO BE
REDUCED BY ROW SCALING. FOR UNBALANCED
MATRICES SET L = N.
- INPUT SCALAR CONTAINING THE ORDER OF
THE MATRIX TO BE REDUCED.
- INPUT SCALAR CCNTAINING ROW DIMENSION
OF AR AND AI IN THE CALLING PROGRAM.
- OUTPUT VECTOR OF LENGTH L CONTAINING
DETAILS OF THE TRANSFORMATIONS.
- SINGLE/DOUBLE

PRECISION

EBAC1370
EBAC1380
EBAC1390
EBAC1400
EBAC1410
EBAC1420
EBAC1430
EBAC1440
EBAC1450
EBAC1460
EBAC1470
EBAC1480
EBAC1490

EHEC0010
EHEC0020
EHEC0030
EHEC0040
EHEC0050
EHEC0060
EHEC0070
EHEC0080
EHEC0090
EHEC0100
EHEC0110
EHEC0120
EHEC0130
EHEC0140
EHEC0150
EHEC0160
EHEC0170
EHEC0180
EHEC0190
EHEC0200
EHEC0210
EHEC0220
EHEC0230
EHEC0240
EHEC0250
EHEC0260
EHEC0270
EHEC0280
EHEC0290
EHEC0300
EHEC0310
EHEC0320
EHEC0330
EHEC0340


```

C      LANGUAGE      - FORTRAN
C-----
C      LATEST REVISION - FEBRUARY 7, 1973
C
C      SUBROUTINE EHESSC (AR, AI, K, L, N, IA, ID)
C
C      DIMENSION
C      DOUBLE PRECISION
C      COMPLEX*16
C      EQUIVALENCE
C
C      DATA
C      LA=L-1
C      KPI=K+1
C      IF (LA .LT. KPI) GO TO 45
C      DC 40 M=KPI,LA
C      I=M
C      XR=ZERO
C      XI=ZERO
C      DO 5 J=M,L
C      IF (DABS(AR(J,M-1))+DABS(AI(J,M-1))) .LE. DABS(XR)+DABS(XI))
C      1 GO TO 5
C      XR=AR(J,M-1)
C      XI=AI(J,M-1)
C      I=J
C      CONTINUE
C      ID(M)=I
C      IF (I .EQ. M) GO TO 20
C
C      MM1=M-1
C      DO 10 J=MM1,N
C      YR=AR(I,J)
C      AR(I,J)=AR(M,J)
C      AR(M,J)=YR
C      YI=AI(I,J)
C      AI(I,J)=AI(M,J)
C      AI(M,J)=YI
C      CONTINUE
C      DO 15 J=1,L
C      YR=AR(J,I)
C      AR(J,I)=AR(J,M)
C      AR(J,M)=YR
C      YI=AI(J,I)
C      AI(J,I)=AI(J,M)
C      AI(J,M)=YI
C      CONTINUE
C      15
C
C      INTERCHANGE ROWS AND COLUMNS OF
C      ARRAYS AR AND AI
C
C      END INTERCHANGE
C
EHEC0350
EHEC0360
EHEC0370
EHEC0380
EHEC0390
EHEC0400
EHEC0410
EHEC0420
EHEC0430
EHEC0450
EHEC0460
EHEC0470
EHEC0490
EHEC0500
EHEC0510
EHEC0520
EHEC0530
EHEC0540
EHEC0550
EHEC0560
EHEC0570
EHEC0580
EHEC0610
EHEC0620
EHEC0630
EHEC0640
EHEC0650
EHEC0660
EHEC0670
EHEC0680
EHEC0690
EHEC0700
EHEC0710
EHEC0720
EHEC0730
EHEC0740
EHEC0750
EHEC0760
EHEC0770
EHEC0780
EHEC0790
EHEC0800
EHEC0810
EHEC0820
EHEC0830
EHEC0840
EHEC0850
EHEC0860

```



```

20 IF (XR .EQ. ZERO .AND. XI .EQ. ZERO) GO TO 40
   MP1=M+1
   DO 35 I=MPL,L
     YR=AR(I,M-1)
     YI=AI(I,M-1)
     IF (YR .EQ. ZERO .AND. YI .EQ. ZERO) GO TO 35
     Y=Y/X
     AR(I,M-1)=YR
     AI(I,M-1)=YI
     DO 25 J=M,N
       CONTINUE
     DO 30 J=1,L
       AR(J,M)=YR*AR(J,I)-YI*AI(J,I)
       AI(J,M)=YI*AR(J,I)+YR*AI(J,I)
       CONTINUE
     CONTINUE
   CONTINUE
30 RETURN
35 CONTINUE
40 CONTINUE
45 END

```

EHEC0870
 EHEC0880
 EHEC0890
 EHEC0900
 EHEC0910
 EHEC0920
 EHEC0930
 EHEC0940
 EHEC0970
 EHEC0950
 EHEC0980
 EHEC0960
 EHEC0990
 EHEC1000
 EHEC1010
 EHEC1020
 EHEC1030
 EHEC1040
 EHEC1050
 EHEC1060
 EHEC1070

```

C-----D-----LIBRARY 1-----
SUBROUTINE ELRH2C (HR,HI,K,L,N,IH,WR,WI,ZR,ZI,ID,INFER,IER)

FUNCTION
  - COMPUTE THE EIGENVALUES AND EIGENVECTORS OF
  - A COMPLEX UPPER HESSENBERG MATRIX AND
  - BACK TRANSFORM THE EIGENVECTORS.
  - CALL ELRH2C (HR,HI,K,L,N,IH,WR,WI,ZR,ZI,ID,
  - INFER,IER)
  - INPUT MATRIX OF DIMENSION N BY N CONTAINING
  - THE REAL COMPONENTS OF THE COMPLEX
  - HESSENBERG MATRIX. HR IS DESTROYED ON
  - OUTPUT.
  - INPUT MATRIX OF DIMENSION N BY N CONTAINING
  - THE IMAGINARY COUNTERPARTS TO HR, ABOVE.
  - HI IS DESTROYED ON OUTPUT.
  - INPUT SCALAR CONTAINING THE LOWER BOUNDARY
  - INDEX FOR THE INPUT MATRIX.
  - FOR UNBALANCED MATRICES SET K = 1.
  - INPUT SCALAR CONTAINING THE UPPER BOUNDARY
  - INDEX FOR THE INPUT MATRIX.
  - FOR UNBALANCED MATRICES SET L = N.
  - INPUT SCALAR CONTAINING THE ORDER OF THE
  - HESSENBERG MATRIX AND THE EIGENVECTOR
  - MATRIX.

PARAMETERS HR HI K L N

ELRH2C-----D-----LIBRARY 1-----

```

ELR20010
 ELR20020
 ELR20030
 ELR20040
 ELR20050
 ELR20060
 ELR20070
 ELR20080
 ELR20090
 ELR20100
 ELR20110
 ELR20120
 ELR20130
 ELR20140
 ELR20150
 ELR20160
 ELR20170
 ELR20180
 ELR20190
 ELR20200
 ELR20210
 ELR20220
 ELR20230
 ELR20240
 ELR20250

IH - INPUT SCALAR CONTAINING THE ROW DIMENSION
 OF MATRICES HR, HI, ZR AND ZI IN THE
 CALLING PROGRAM.
 WR - OUTPUT VECTOR OF LENGTH N CONTAINING THE REAL
 COMPONENTS OF THE EIGENVALUES.
 WI - OUTPUT VECTOR OF LENGTH N CONTAINING THE
 IMAGINARY COMPONENTS OF THE EIGENVALUES.
 ZR - OUTPUT MATRIX OF DIMENSION N BY N CONTAINING
 THE REAL COMPONENTS OF THE EIGENVECTORS.
 ZI - OUTPUT MATRIX OF DIMENSION N BY N CONTAINING
 THE EIGENVECTORS ARE NOT NORMALIZED.
 ID - INPUT VECTOR OF DIMENSION N BY N CONTAINING
 THE IMAGINARY COUNTERPARTS TO ZR, ABOVE.
 INFER - OUTPUT SCALAR CONTAINING THE INDEX OF THE
 EIGENVALUE WHICH GENERATED THE TERMINAL
 ERROR (SEE DESCRIPTION OF IER, BELOW).
 IER - ERROR PARAMETER

TERMINAL ERROR = 128 + N INDICATES THE EIGENVALUE RECORDED
 IN THE OUTPUT PARAMETER, INFER,
 COULD NOT BE DETERMINED AFTER 30
 ITERATIONS. IF THE J-TH EIGENVALUE
 COULD NOT BE SO DETERMINED,
 THEN THE EIGENVALUES J+1, J+2, ..., N
 SHOULD BE CORRECT.

PRECISION - SINGLE/DOUBLE
 REQD. IMSL ROUTINES - UERTST
 LANGUAGE - FORTRAN

LATEST REVISION - APRIL 5, 1977

SUBROUTINE ELRH2C (HR, HI, K, L, N, IH, WR, WI, ZR, ZI, ID, INFER, IER)

DIMENSION
 DIMENSION
 COMPLEX*16
 DOUBLE PRECISION
 DOUBLE PRECISION
 DOUBLE PRECISION
 EQUIVALENCE
 (X, T1(1), XRI), (T1(2), XI),
 (Y, T2(1), YRI), (T2(2), YI),
 (Z, T3(1), ZRI), (T3(2), ZI),
 ZERO, ONE, TWO/0.000, 1.000, 2.000/
 DATA

ELR20260
 ELR20270
 ELR20280
 ELR20290
 ELR20300
 ELR20310
 ELR20320
 ELR20330
 ELR20340
 ELR20350
 ELR20360
 ELR20370
 ELR20380
 ELR20390
 ELR20400
 ELR20410
 ELR20420
 ELR20430
 ELR20440
 ELR20450
 ELR20460
 ELR20470
 ELR20480
 ELR20490
 ELR20500
 ELR20510
 ELR20520
 ELR20530
 ELR20540
 ELR20550
 ELR20560
 ELR20570
 ELR20580
 ELR20590
 ELR20600
 ELR20610
 ELR20620
 ELR20630
 ELR20640
 ELR20650
 ELR20660
 ELR20680
 ELR20690
 ELR20700
 ELR20710
 ELR20720
 ELR20730
 ELR20740

EPS/Z3410000000000000/
INITIALIZE IER

ELR20750
ELR20770
ELR20780
ELR20790
ELR20800
ELR20810
ELR20820
ELR20830
ELR20840
ELR20850
ELR20860
ELR20870
ELR20880
ELR20890
ELR20900
ELR20910
ELR20920
ELR20930
ELR20940
ELR20950
ELR20960
ELR20970
ELR20980
ELR20990
ELR21000
ELR21010
ELR21020
ELR21030
ELR21040
ELR21050
ELR21060
ELR21070
ELR21080
ELR21090
ELR21100
ELR21110
ELR21120
ELR21130
ELR21140
ELR21150
ELR21160
ELR21170
ELR21180
ELR21190
ELR21200
ELR21210
ELR21220
ELR21230

```

C      DATA
      IER=0
      INFER=0
      TR=ZERO
      TI=ZERO
      DC 5 I=1,N
      DO 3 J=1,N
        ZR(I,J)=ZERO
        ZI(I,J)=ZERO
      3   CONTINUE
      ZR(I,I) = ONE
      5   CONTINUE

      IEND=L-K-1
      IF (IEND .LE. 0) GO TO 25

      DO 20 II=1,IEND
        I=L-II
        IP1=I+1
        IM1=I-1
        DO 10 M=IP1,L
          ZR(M,I)=HR(M,IM1)
          ZI(M,I)=HI(M,IM1)
        10  CONTINUE
        J=ID(I)
        IF (I .EQ. J) GO TO 20
        DO 15 M=I,L
          ZR(I,M)=ZR(J,M)
          ZI(I,M)=ZI(J,M)
          ZR(J,M)=ZERO
          ZI(J,M)=ZERO
        15  CONTINUE
        ZR(J,I)=ONE
      20  CONTINUE
      DO 30 I=1,N
        IF (I .GE. K .AND. I .LE. L) GO TO 30
        WR(I)=HR(I,I)
        WI(I)=HI(I,I)
      30  CONTINUE
      NN=L

      SEARCH FOR NEXT EIGENVALUE

      35 IF (NN .LT. K) GO TO 150
      ITS=0
      NNM1=NN-1
      NNM2=NN-2

```



```

C      IF (NN .EQ. K) GO TO 50
C      LOOK FOR SINGLE SMALL SUB-DIAGONAL
C      ELEMENT
C      DO M=NN,K+1,-1
C      DO 45 KK=K,NNM1
C      M=NPL-KK
C      MM1=M-1
C      IF (DABS(HR(M,MM1))+DABS(HI(M,MM1))) .LE. EPS*(DABS(HR(MM1,MM1))) GO TO 55
C      1
C      45 CONTINUE
C      50 M=K
C      55 IF (M .EQ. NN) GO TO 145
C      IF (ITS .EQ. 30) GO TO 205
C      IF (ITS .EQ. 10 .OR. ITS .EQ. 20) GO TO 60
C      SR=HR(NN,NN)
C      SI=HI(NN,NN)
C      XR=HR(NN,NNM1)-HI(NN,NNM1,NN)*HI(NN,NNM1)
C      XI=HR(NN,NNM1,NN)*HI(NN,NNM1,NN)+HI(NN,NNM1,NN)*HR(NN,NNM1)
C      IF (XR .EQ. ZERO .AND. XI .EQ. ZERO) GO TO 65
C      YR=(HR(NN,NNM1,NN)-SR)/TWO
C      YI=(HI(NN,NNM1,NN)-SI)/TWO
C      Z=CDOSQRT(DCMPLX(YR**2-YI**2+XR,TWO*YR*YI+XI))
C      IF (YR*ZZR+YI*ZZI .LT. ZERO) Z=-Z
C      X=X/(Y+Z)
C      SR=SR-XR
C      SI=SI-XI
C      GO TO 65
C      60 SR=DABS(HR(NN,NNM1))+DABS(HR(NN,NNM1,NNM2))
C      SI=DABS(HI(NN,NNM1))+DABS(HI(NN,NNM1,NNM2))
C      65 DO 70 I=K,NN
C      HR(I,I)=HR(I,I)-SR
C      HI(I,I)=HI(I,I)-SI
C      70 CONTINUE
C      TR=TR+SR
C      TI=TI+SI
C      ITS=ITS+1
C      LOOK FOR TWO CONSECUTIVE SMALL
C      SUB-DIAGONAL ELEMENTS
C      XR=DABS(HR(NN,NNM1,NNM1))+DABS(HI(NN,NNM1,NNM1))
C      YR=DABS(HR(NN,NNM1,NNM1))+DABS(HI(NN,NNM1,NNM1))
C      ZZR=DABS(HR(NN,NNM1,NNM1))+DABS(HI(NN,NNM1,NNM1))
C      NNMJ=NNM1-M
C      IF (NNMJ .EQ. 0) GO TO 80
C      DO MM=NN-1,M+1,-1
C      DO 75 NM=1,NNMJ
C      MM=NN-NM

```

ELR21240
ELR21250
ELR21260
ELR21270
ELR21280
ELR21290
ELR21300
ELR21310
ELR21320
ELR21330
ELR21360
ELR21370
ELR21380
ELR21390
ELR21400
ELR21410
ELR21420
ELR21430
ELR21440
ELR21450
ELR21460
ELR21470
ELR21480
ELR21490
ELR21510
ELR21520
ELR21530
ELR21540
ELR21550
ELR21560
ELR21570
ELR21600
ELR21610
ELR21620
ELR21630
ELR21640
ELR21650
ELR21660
ELR21670
ELR21680
ELR21690
ELR21700
ELR21710
ELR21750
ELR21760
ELR21770
ELR21780
ELR21790


```

MMM1=MM-1
YI=YR
YR=DABS(HR(MM,MMM1))+DABS(HI(MM,MMM1))
XI=ZZR
ZZR=XR
XR=DABS(HR(MMM1,MMM1))+DABS(HI(MMM1,MMM1))
IF (YR .LE. EPS*ZZR/YI*(ZZR+XR+XI)) GO TO 85
75 CONTINUE
80 MM=M
C
85 MP1=MM+1
DO 110 I=MP1,NN
IM1=I-1
XR=HR(IM1,IM1)
XI=HI(IM1,IM1)
YR=HR(I,IM1)
YI=HI(I,IM1)
IF (DABS(XR)+DABS(XI) .GE. DABS(YR)+DABS(YI)) GO TO 95
INTERCHANGE ROWS OF HR AND HI
DO 90 J=IM1,N
ZZR=HR(IM1,J)
HR(IM1,J)=HR(I,J)
HR(I,J)=ZZR
ZZI=HI(IM1,J)
HI(IM1,J)=HI(I,J)
HI(I,J)=ZZI
CONTINUE
90 Z=X/Y
WR(I)=ONE
GO TO 100
95 Z=Y/X
WR(I)=-ONE
WR(I,IM1)=ZZR
HI(I,IM1)=ZZI
DO 105 J=I,N
HR(I,J)=HR(I,J)-ZZR*HR(IM1,J)+ZZI*HI(IM1,J)
HI(I,J)=HI(I,J)-ZZR*HI(IM1,J)+ZZI*HR(IM1,J)
CONTINUE
105 CONTINUE
110 COMPOSITION R*L=H
C
DO 140 J=MP1,NN
JM1=J-1
XR=HR(J,JM1)
XI=HI(J,JM1)
HR(J,JM1)=ZERO
HI(J,JM1)=ZERO
C
C
INTERCHANGE COLUMNS OF HR, HI,
ZR, AND ZI IF NECESSARY

```


IF (WR(J).LE. ZERO) GO TO 125

DO 115 I=1,J
 ZZR=HR(I,JM1)
 HR(I,JM1)=HR(I,J)
 HR(I,J)=ZZR
 ZZI=HI(I,JM1)
 HI(I,JM1)=HI(I,J)
 HI(I,J)=ZZI

CONTINUE

115

DO 120 I=K,L
 ZZR=ZR(I,JM1)
 ZR(I,JM1)=ZR(I,J)
 ZR(I,J)=ZZR
 ZZI=ZI(I,JM1)
 ZI(I,JM1)=ZI(I,J)
 ZI(I,J)=ZZI

CONTINUE

120

END INTERCHANGE COLUMNS

DO 130 I=1,J
 HR(I,JM1)=HR(I,JM1)+XR*HR(I,J)-XI*HI(I,J)
 HI(I,JM1)=HI(I,JM1)+XR*HI(I,J)+XI*HR(I,J)

CONTINUE

130

DO 135 I=K,L
 ZR(I,JM1)=ZR(I,JM1)+XR*ZR(I,J)-XI*ZI(I,J)
 ZI(I,JM1)=ZI(I,JM1)+XR*ZI(I,J)+XI*ZR(I,J)

CONTINUE

135

END ACCUMULATE TRANSFORMATIONS

CONTINUE
 GC TO 40

C

A ROOT FOUND

145 WR(NN)=HR(NN,NN)+TR
 WI(NN)=HI(NN,NN)+TI
 NN=NNMI
 GO TO 35

C

ALL ROOTS FOUND. BACKSUBSTITUTE TO
 FIND VECTORS OF UPPER TRIANGULAR
 FORM

150 IF (N.EQ. 1) GO TO 9005
 FNORM=ZERO
 DC 160 I=1,N
 FNORM=FNORM+DABS(WR(I))+DABS(WI(I))
 IF (I.EQ. N) GO TO 160
 IPI=I+1
 DO 155 J=IPI,N
 FNORM=FNORM+DABS(HR(I,J))+DABS(HI(I,J))

CONTINUE

155

CONTINUE

160 IF (FNORM .EQ. ZERO) GO TO 9005

ELR22310
 ELR22320
 ELR22330
 ELR22340
 ELR22350
 ELR22360
 ELR22370
 ELR22380
 ELR22390
 ELR22400
 ELR22410
 ELR22420
 ELR22430
 ELR22440
 ELR22450
 ELR22460
 ELR22470
 ELR22480
 ELR22490
 ELR22500
 ELR22510
 ELR22520
 ELR22530
 ELR22540
 ELR22550
 ELR22560
 ELR22570
 ELR22580
 ELR22590
 ELR22600
 ELR22610
 ELR22620
 ELR22630
 ELR22640
 ELR22650
 ELR22660
 ELR22670
 ELR22680
 ELR22690
 ELR22700
 ELR22710
 ELR22720
 ELR22730
 ELR22740
 ELR22750
 ELR22760
 ELR22780
 ELR22790
 ELR22800


```

C      NP2 = N+2
C      DO 180 NM=2,N
      NN=NP2-NM
      XR=WR(NN)
      XI=WI(NN)
      NAM1=NN-1
C
C      DO 175 II=1,NNM1
      I=NN-II
      ZZR=HR(I,NN)
      ZZI=HI(I,NN)
      IF (I.EQ. NNM1) GO TO 170
      IP1=I+1
      DO 165 J=IP1,NNM1
      ZZR=ZZR+HR(I,J)*HR(I,J)*HI(I,J)*HI(I,J)
      ZZI=ZZI+HR(I,J)*HI(I,J)*HI(I,J)*HR(I,J)
C      CONTINUE
      YR=XR-WR(I)
      YI=XI-WI(I)
      IF (YR.EQ. ZERO .AND. YI.EQ. ZERO) YR=EPS*FNORM
      Z=Z/Y
      HR(I,NN)=T3(1)
      HI(I,NN)=T3(2)
C      CONTINUE
C      CONTINUE
C      NMI=N-1
C      DO 190 I=1,NMI
      IF (I.GE. K .AND. I.LE. L) GO TO 190
      IP1=I+1
      DO 185 J=IP1,N
      ZR(I,J)=HR(I,J)
      ZI(I,J)=HI(I,J)
C      CONTINUE
C      CONTINUE
      IF (L.EQ. 0) GO TO 9005
C
C      NPL=N+K
C      DO 200 JJ=K,NMI
      J=NPL-JJ
      JM1=J-1
      DO 200 I=K,L
      ZZR=ZR(I,J)

```


ELR233290
ELR233300
ELR233310
ELR233320
ELR233330
ELR233340
ELR233350
ELR233360
ELR233370
ELR233380
ELR233390
ELR233400
ELR233410
ELR233420
ELR233430
ELR233440
ELR233450
ELR233460
ELR233470

```

ZZI=ZI(I,J)
MM=JMI
IF (L.LT. J) MM=L
DO 195 M=K,MM
  ZZR=ZZR+ZR(I,M)*HR(M,J)-ZI(I,M)*HI(M,J)
  ZZI=ZZI+ZR(I,M)*HI(M,J)+ZI(I,M)*HR(M,J)
CONTINUE
ZR(I,J)=ZZR
ZI(I,J)=ZZI
200 CONTINUE
GO TO 9005

195
200 CONTINUE
GO TO 9005

205 IER=129
INFER=NN
CONTINUE
9000 CALL UERTST (IER,6ELRH2C)
9005 RETURN
END

```

SET ERROR - NO CONVERGENCE TO AN
EIGENVALUE AFTER 30 ITERATIONS

EBBC0010
EBBC0020
EBBC0030
EBBC0040
EBBC0050
EBBC0060
EBBC0070
EBBC0080
EBBC0090
EBBC0100
EBBC0110
EBBC0120
EBBC0130
EBBC0140
EBBC0150
EBBC0160
EBBC0170
EBBC0180
EBBC0190
EBBC0200
EBBC0210
EBBC0220
EBBC0230
EBBC0240
EBBC0250
EBBC0260
EBBC0270

```

SUBROUTINE EBBCKC (ZR,ZI,N,IZ,K,L,M,D)
C-----D-----LIBRARY 1-----
C
C FUNCTION
C
C USAGE
C
C PARAMETERS
C
C ZR
C
C ZI
C
C N
C
C IZ
C
C K
C
C L
C
C M
C
C D
C
C - BACKTRANSFORM THE EIGENVECTORS OF A BALANCED
C   COMPLEX GENERAL MATRIX.
C - CALL EBBCKC (ZR,ZI,N,IZ,K,L,M,D)
C - INPUT/OUTPUT MATRICES OF DIMENSION N BY M.
C   ON INPUT, THE FIRST M COLUMNS OF ZR AND
C   ZI CONTAIN THE REAL AND IMAGINARY PARTS,
C   RESPECTIVELY, OF THE EIGENVECTORS TO BE
C   BACK TRANSFORMED. ON OUTPUT, THESE M
C   COLUMNS CONTAIN THE REAL AND IMAGINARY
C   PARTS OF THE TRANSFORMED EIGENVECTORS.
C - INPUT SCALAR CONTAINING THE NUMBER OF
C   ROWS IN THE MATRIX Z = (ZR,ZI). N MUST
C   NOT BE GREATER THAN IZ.
C - INPUT SCALAR CONTAINING THE ROW DIMENSION
C   OF MATRICES ZR AND ZI IN THE CALLING
C   PROGRAM.
C - INPUT SCALARS CONTAINING THE BOUNDARY
C   INDICES FOR THE BALANCED MATRIX. K AND L
C   ARE TWO OUTPUT PARAMETERS FROM IMSL ROUTINE
C   EBALAC.
C - INPUT SCALAR CONTAINING THE NUMBER OF COLUMNS
C   OF Z = (ZR,ZI) TO BE BACK TRANSFORMED.
C - INPUT VECTOR OF LENGTH N CONTAINING THE

```


C	PRECISION	DETAILS OF THE TRANSFORMATIONS PRODUCED	EBBC0280
C	LANGUAGE	BY IMSL ROUTINE EBALAC.	EBBC0290
C		- SINGLE/DOUBLE	EBBC0300
C		- FORTRAN	EBBC0310
C	LATEST REVISION	- MARCH 9, 1977	EBBC0320
C			EBBC0330
C	SUBROUTINE EBBCKC (ZR,ZI,N,IZ,K,L,M,D)		EBBC0340
C			EBBC0350
C			EBBC0360
C	DIMENSION	ZR(IZ,1),ZI(IZ,1),D(1)	EBBC0370
C	DOUBLE PRECISION	ZR,ZI,D,S	EBBC0380
C	IF (L.EC.K) GO TO 15		EBBC0390
C	DO 10 I = K,L		EBBC0400
C	S = D(I)		EBBC0410
C		LEFT HAND EIGENVECTORS ARE BACK	EBBC0420
C		TRANSFORMED IF THE ABOVE	EBBC0430
C		STATEMENT IS REPLACED BY S=1.0/D(I)	EBBC0440
C			EBBC0450
C			EBBC0460
C			EBBC0470
C			EBBC0480
C			EBBC0490
C			EBBC0500
C			EBBC0510
C			EBBC0520
C			EBBC0530
C			EBBC0540
C			EBBC0550
C			EBBC0560
C			EBBC0570
C			EBBC0580
C			EBBC0590
C			EBBC0600
C			EBBC0610
C			EBBC0620
C			EBBC0630
C			EBBC0640
C			EBBC0650
C			EBBC0660
C			EBBC0670
C			EBBC0680


```

10 CONTINUE
5 CONTINUE
15 DO 25 I = 1,N
  I = II
  IF (I.GE.K.AND.I.LE.L) GO TO 25
  IF (I.LT.K) I = K-II
  KK = D(I)
  IF (KK.EQ.I) GO TO 25
  DO 20 J = 1,M
    S = ZR(I,J)
    ZR(I,J) = ZR(KK,J)
    ZR(KK,J) = S
    S = ZI(I,J)
    ZI(I,J) = ZI(KK,J)
    ZI(KK,J) = S
  20 CONTINUE
25 CONTINUE
RETURN
END

```



```

DO 25 I=K-1,1,-1 AND
DO I=L+1,N,1

```



```

SUBROUTINE UERTST ( IER,NAME )
-----LIBRARY 1-----
FUNCTION
- ERROR MESSAGE GENERATION

```


C	UERTST	UERT0010
C		UERT0020
C		UERT0030
C		UERT0040
C		UERT0050


```

//EIG$FCN JOB (1719,0947,AX74),SMC 1882',TIME=2
//EXEC FORTCLGW
//FORT.SYSIN DD *
.....
PROGRAM EIGFCN
PERTURBATION VELOCITY PLOT PROGRAM
NI = 0
.....
PURPOSE
.....
TO PLOT THE NONDIMENSIONALIZED PERTURBATION VELOCITY U AGAINST
NONDIMENSIONALIZED RADIUS UTILIZING THE DATA GENERATED
BY PROGRAM PIPEO (MODE=1). PLOTTING IS PERFORMED ON
THE NPS VERSATEC PLOTTER USING SUBROUTINE PLOTG.
.....
IMPLICIT REAL*8(A-H,O-Z)
COMPLEX *16QPRIM(85),DQPRIM(85),ALPHA,UP(85),UPPRIM(85),CONST,GAMMA
1A
REAL *8ETA(85),U(85),UR(85),UI(85)
REAL *4URI(85),U1I(85),RAD1(85),SREY,SLAMDA,SGAMMA,AR,AI
READ N,REY,ALPHA,LAMBDA,GAMMA & QPRIME'S
READ (5,6) N,REY,ALPHA
NO = N+1
N1 = N+2
READ (5,7) AMDA,GAMMA
READ (5,8) KSET
SLAMDA = AMDA
SREY = REY
AR = ALPHA
AI = AIMAG(ALPHA)
SGAMMA = GAMMA
SGAMMA = SGAMMA + AR
.....
DC 1 I=2,NO
READ (5,9) ETA(I),QPRIM(I)
1 CONTINUE
.....

```



```

C      COMPUTE UPPRIME'S
C      DEL = 1.00/DFLOAT(N+1)
C      ETA(1) = 0.000
C      QPRIM(1) = 1.79591836700*QPRIM(2)-1.2478134100*QPRIM(3)+0.60641399
C      14000*QPRIM(4)-0.17784256600*QPRIM(5)+0.02332361500*QPRIM(6)
C      UPPRIM(1) = 200*QPRIM(1)
C      CALL COEFNT (ETA(2),AMDA,COEF,KSET)
C      DQPRIM(2) = 200*(-QPRIM(2)+QPRIM(3))/(300*DEL)
C      DQPRIM(2) = COEF*DQPRIM(2)
C      UPPRIM(2) = 200*QPRIM(2)+ETA(2)*DQPRIM(2)
C      CALL COEFNT (ETA(3),AMDA,COEF,KSET)
C      DQPRIM(3) = 400*(-QPRIM(2)+QPRIM(3))/(300*DEL)
C      DQPRIM(3) = COEF*DQPRIM(3)
C      UPPRIM(3) = 200*QPRIM(3)+ETA(3)*DQPRIM(3)
C      DO 2 I=4,N
C      CALL COEFNT (ETA(I),AMDA,COEF,KSET)
C      DQPRIM(I) = (QPRIM(I+1)-QPRIM(I-1))/(200*DEL)
C      DQPRIM(I) = COEF*DQPRIM(I)
C      UPPRIM(I) = 200*QPRIM(I)+ETA(I)*DQPRIM(I)
C      2 CONTINUE
C      CALL COEFNT (ETA(N0),AMDA,COEF,KSET)
C      DQPRIM(N0) = -QPRIM(N)/(200*DEL)
C      DQPRIM(N0) = COEF*DQPRIM(N0)
C      UPPRIM(N0) = 200*QPRIM(N0)+ETA(N0)*DQPRIM(N0)
C      ETA(N1) = 1.000
C      UPPRIM(N1) = (000,000)
C      WRITE (6,10)
C      DETERMINE U VECTOR OF LARGEST MAGNITUDE
C      C = 0.00
C      DO 3 I=1,N1
C      IF (CDABS(UPPRIM(I)).GT.C) INDEX=I
C      IF (CDABS(UPPRIM(I)).GT.C) C=CDABS(UPPRIM(I))
C      3 CONTINUE
C      CONST = DCONJG(UPPRIM(INDEX))/C**2

```



```
C C C C C
NORMALIZE UPRIMES'S AND SPLIT INTO REAL & IMAGINARY VECTORS
C C C C C
DO 4 I=1,N1
UP(I) = CONST*UPRIM(I)
UR(I) = UP(I)
UI(I) = (OD0,-1D0)*UP(I)
4 CONTINUE
C C C C C
CONVERT U'S AND ETA'S TO SINGLE PRECISION FCR PLOTG
C C C C C
DO 5 I=1,N1
RAD1(I) = ETA(I)
UR1(I) = UR(I)
UI1(I) = UI(I)
WRITE(6,I1) RAD1(I),UR1(I),UI1(I)
5 CONTINUE
C C C C C
PLOT RESULTS
CALL PLOTG(RAD1,UR1,N1,1,1,1,'RADIUS',6,'PERTURBATION VELOCITY',
$ 21,0,1,1,1,7,7.)
CALL PLOTG(RAD1,UI1,N1,2,1,5,'RADIUS',6,'PERTURBATION VELOCITY',
$ 21,0,1,1,1,7,7.)
CALL CHART(N,SREY,AR,AI,SGAMMA,SLAMDA)
CALL PLOT(0.0,0.0,999)
STOP
C C C C C
6 FORMAT (I2,3D20.10)
7 FORMAT (F15.7,2(1PD20.10))
8 FORMAT (I2)
9 FORMAT (F15.7,2(1PD20.10))
10 FORMAT (.1,)
11 FORMAT (. , ,3F15.7)
END
C C C C C
.....SUBROUTINE COEFNT(ETA,AMDA,COEF,KSET).....COEFF
COEFF
COEFF
COEFF
COEFF
COEFF
COEFF
PURPOSE--WHEN AN OFFSET MESH IS USED, THIS SUBROUTINE GENERATES
THE COEFFICIENT REQUIRED TO CONVERT DQ/DETA TO DQ/DR AND
CONVERTS THE UNIFORM ETA VALUE INTO THE NONUNIFORM R VALUE
C C C C C
```



```

3 COEF = 1D0
  RETURN
  END
COEF 560
COEF 570
COEF 580

.....SUBROUTINE CHART(N,SREY,AR,AI,SGAMMA,SLAMDA).....
CHAR 10
CHAR 20
CHAR 30
CHAR 40
CHAR 50
CHAR 60
CHAR 70
CHAR 80
CHAR 90
CHAR 100
CHAR 110
CHAR 120
CHAR 130
CHAR 140
CHAR 150
CHAR 160
CHAR 170
CHAR 180
CHAR 190
CHAR 200
CHAR 210
CHAR 220
CHAR 230
CHAR 240
CHAR 250
CHAR 260
CHAR 270
CHAR 280
CHAR 290
CHAR 300
CHAR 310
CHAR 320
CHAR 330
CHAR 340
CHAR 350
CHAR 360
CHAR 370
CHAR 380
CHAR 390
CHAR 400
CHAR 410
CHAR 420
CHAR 430

PURPOSE
  TO LABEL THE GRAPH WITH INFORMATION PERTAINING TO THE PLOT

EXAMPLE OF THE CALLING ARGUMENT
  CALL CHART(N,SREY,AR,AI,SGAMMA,SLAMDA)

DESCRIPTION OF PARAMETERS
  THE PARAMETERS ARE SELF-EXPLANATORY AND MUST BE IN SINGLE
  PRECISION FOR PLOTTING.

OTHER SUBROUTINES NEEDED
  ONLY BUILT-IN VERSATEC PLOTTING FUNCTIONS NEWPEN,SYMBOL &
  NUMBER. NOTE THAT THESE ROUTINES MAY ONLY BE
  ACCESSED WHEN RUNNING UNDER 'FORTCLGW'.

.....
SUBROUTINE CHART (N,SREY,AR,AI,SGAMMA,SLAMDA)
CC
CC
  X0 = 2.5
  Y0 = 6.5
  HT = 0.15
  HT1 = 0.7*HT
  DELY1 = .08*HT
  DELY2 = .065*HT1
  DELX = .1
  GRAPH TITLE
CC
CC
  CALL NEWPEN (2)
  CALL SYMBOL(X0,Y0,HT,'NORMALIZED PERTURBATION VELOCITY',0.,32)

```



```

C
C
C
X0 = X0+7.*DELX
Y0 = Y0-DELY1
CALL SYMBOL(X0,Y0,HT,'FOR THE CASE N = 0',0.,18)
MESH VALUE
CALL NEWPEN (1)
X0 = X0+4.*DELX
Y0 = Y0-DELY1
SN = FLOAT(N)
CALL SYMBOL(X0,Y0,HT1,'NMESH = ',0.,9)
CALL NUMBER (999.,999.,HT1,SN,0.,-1)
REY VALUE
YC = Y0-DELY2
CALL SYMBOL(X0,Y0,HT1,'REY
CALL NUMBER (999.,999.,HT1,SREY,0.,-1)
ALPHA VALUE
X1 = X0+11.*DELY2
Y0 = Y0-DELY2
CALL SYMBOL(X0,Y0,HT1,'ALPHA = ',0.,9)
CALL NJMBER (999.,999.,HT1,AR,0.,1)
CALL NUMBER (X1,Y0,HT1,AI,0.,1)
GAMMA RL* VALUE
Y0 = Y0-DELY2
CALL SYMBOL(X0,Y0,HT1,'GAMMA* = ',0.,9)
CALL NUMBER (999.,999.,HT1,SGAMMA,0.,4)
LAMBDA VALUE
Y0 = Y0-DELY2
CALL SYMBOL(X0,Y0,HT1,'LAMBDA = ',0.,9)
CALL NUMBER (999.,999.,HT1,SLAMDA,0.,1)
SYMBOL LEGEND
Y0 = 1.75
CALL SYMBOL(X0,Y0,HT1,'OCTAGON = U(REAL)',0.,17)
Y0 = Y0-DELY2
CALL SYMBOL(X0,Y0,HT1,'DIAMOND = U(IMAG)',0.,17)
RETURN
END
C

```

```

CHAR 440
CHAR 450
CHAR 460
CHAR 470
CHAR 480
CHAR 490
CHAR 500
CHAR 510
CHAR 520
CHAR 530
CHAR 540
CHAR 550
CHAR 560
CHAR 570
CHAR 580
CHAR 590
CHAR 600
CHAR 610
CHAR 620
CHAR 630
CHAR 640
CHAR 650
CHAR 660
CHAR 670
CHAR 680
CHAR 690
CHAR 700
CHAR 710
CHAR 720
CHAR 730
CHAR 740
CHAR 750
CHAR 760
CHAR 770
CHAR 780
CHAR 790
CHAR 800
CHAR 810
CHAR 820
CHAR 830
CHAR 840
CHAR 850
CHAR 860
CHAR 870
CHAR 880
CHAR 890
CHAR 900

```


.....
THE FOLLOWING CARDS COMPRISE THE DATA DECK FOR PROGRAM EIGFCN.

/*
//GO.SYSIN DD *

DATA DECK FROM ONE RUN OF PROGRAM PIPEO (MODENO = 1)

/*
.....


```

//STB$CONT JOB ('1719,0947,AX74'),'SMC 1882',TIME=2
//EXEC FORTCLGW
//FORT.SYSIN DD *
C.....
PROGRAM STBCONT
PURPOSE
TO GENERATE A CONTOUR PLOT CONTAINING LINES OF INCIPIENT,
CRITICAL & FULLY DEVELOPED INSTABILITY USING DATA GENERATED
BY PROGRAM PIPEO (MODENO = 2). THE PLOT IS GENERATED ON THE
NPS VERSATEC PLOTTER USING SUBROUTINE PLOTG WITH ALPHA REAL
ON THE X-AXIS AND ALPHA IMAGINARY ON THE Y-AXIS.
C.....
DIMENSION X1(200), X2(200), X3(200), Y1(200), Y2(200), Y3(200)
COMMON /ARAY/ G1(41,41), AR1(41), AI1(41)
DATA X1,X2,X3,Y1,Y2,Y3/1200*0.0/
SET INITIAL VALUES
READ (5,9) NDIM
XMIN = -.5
XMAX = 0.
YMIN = 0.
YMAX = 10.
THE NEXT 3 VALUES MUST BE SET BY THE USER PRIOR TO RUNNING
THE PROGRAM.
SA = 47.
SREY = 4000.
SLAMDA = 0.0
READ STABILITY MAP VALUES OUTPUT BY PROGRAM PIPEO (MODENO =2)
DO 1 I=1,NDIM
DO 1 J=1,NDIM
READ (5,10) AR1(I),AI1(J),G1(I,J)
1 CONTINUE
COMPUTE POINTS FOR INCIPIENT, CRITICAL & FULLY DEVELOPED
INSTABILITY CURVES.

```



```

C      CALL SEARCH (-1,X1,Y1,NPLT1,NDIM)
C      CALL SEARCH (0,X2,Y2,NPLT2,NDIM)
C      CALL SEARCH (1,X3,Y3,NPLT3,NDIM)
C      JUMP TO PLOT LABEL ROUTINE IF NO INCIPIENT POINTS
C      IF (NPLT1) 8,8,2
C      IF POINTS COMPUTED, NEW PAGE AND WRITE THEM OUT
C      2 WRITE (6,11)
C      DC 3 I=1,NPLT1
C      WRITE (6,12) X1(I),Y1(I)
C      3 CONTINUE
C      PLOT INCIPIENT INSTABILITY POINTS
C      CALL PLOTG(X1,Y1,NPLT1,1,0,1,'ALPHA REAL',10,'ALPHA IMAGINARY',15,
C      $ XMIN,XMAX,YMIN,YMAX,7.,7.)
C      C      LEGEND FOR INCIPIENT SYMBOL
C      CALL NEWPEN (1)
C      CALL SYMBOL (1.3,0.7,.1,'OCTAGON = INCIPIENT INSTABILITY',0.,32)
C      JUMP TO PLOT LABEL ROUTINE IF NO CRITICAL POINTS
C      IF (NPLT2) 8,8,4
C      IF POINTS COMPUTED, NEW PAGE AND PRINT THEM OUT
C      4 WRITE (6,11)
C      DO 5 I=1,NPLT2
C      WRITE (6,12) X2(I),Y2(I)
C      5 CONTINUE
C      PLOT CRITICAL POINTS
C      CALL PLOTG(X2,Y2,NPLT2,2,0,2,'ALPHA REAL',10,'ALPHA IMAGINARY',15,
C      $ XMIN,XMAX,YMIN,YMAX,7.,7.)
C      LEGEND FOR CRITICAL SYMBOL
C

```

```

STBC 460
STBC 470
STBC 480
STBC 490
STBC 500
STBC 510
STBC 520
STBC 530
STBC 540
STBC 550
STBC 560
STBC 570
STBC 580
STBC 590
STBC 600
STBC 610
STBC 620
STBC 630
STBC 640
STBC 650
STBC 660
STBC 670
STBC 680
STBC 690
STBC 700
STBC 710
STBC 720
STBC 730
STBC 740
STBC 750
STBC 760
STBC 770
STBC 780
STBC 790
STBC 800
STBC 810
STBC 820
STBC 830
STBC 840
STBC 850
STBC 860
STBC 870
STBC 880
STBC 890
STBC 900
STBC 910
STBC 920
STBC 930

```


CALL NEWPEN (1)	STBC	940
CALL SYMBOL(1.3,.53,.1,'TRIANGLE = CRITICAL INSTABILITY',0.,31)	STBC	950
JUMP TO PLOT LABEL ROUTINE IF NO FULLY DEVELOPED POINTS	STBC	960
IF (NPLT3) 8,8,6	STBC	970
IF POINTS COMPUTED, NEW PAGE AND PRINT THEM OUT	STBC	980
6 WRITE (6,11)	STBC	990
DC 7 I=1,NPLT3	STBC	1000
WRITE (6,12) X3(1),Y3(1)	STBC	1010
7 CONTINUE	STBC	1020
PLOT FULLY DEVELOPED POINTS	STBC	1030
CALL PLOTG(X3,Y3,NPLT3,3,0,5,'ALPHA REAL',10,'ALPHA IMAGINARY',15,	STBC	1040
\$ XMIN,XMAX,YMIN,YMAX,7.,7.)	STBC	1050
LEGEND FOR FULLY DEVELOPED SYMBOL	STBC	1060
CALL NEWPEN (1)	STBC	1070
CALL SYMBOL(1.3,.36,.1,'DIAMOND = FULLY DEVELOPED INSTABILITY',	STBC	1080
\$ C.,38)	STBC	1090
LABEL THE PLOT	STBC	1100
8 CALL CHART (SN,SREY,SLAMDA)	STBC	1110
CALL PLOT (0.,0.,999)	STBC	1120
STOP	STBC	1130
9 FORMAT (I2)	STBC	1140
10 FORMAT (3E20.10)	STBC	1150
11 FORMAT ('1')	STBC	1160
12 FORMAT ('.',2E20.10)	STBC	1170
END	STBC	1180
	STBC	1190
	STBC	1200
	STBC	1210
	STBC	1220
	STBC	1230
	STBC	1240
	STBC	1250
	STBC	1260
	STBC	1270
	STBC	1280
	STBC	1290
	STBC	1300
	STBC	1310

.....SUBROUTINE SEARCH(NCASE, X, Y,NDIM).....	SEAR	10
PURPOSE	SEAR	20
TO SCAN THE STABILITY MAP FOR CHANGES OF SIGN WITH RESPECT	SEAR	30
TO A SPECIFIED STABILITY VALUE AND GENERATE AN ARRAY OF X,Y	SEAR	40
POINTS DEFINING A CONTOUR OF THE SPECIFIED STABILITY.	SEAR	50
	SEAR	60
	SEAR	70
	SEAR	80

SEAR	11120	90
SEAR	11130	100
SEAR	11140	110
SEAR	11150	120
SEAR	11160	130
SEAR	11170	140
SEAR	11180	150
SEAR	11190	160
SEAR	22200	170
SEAR	22210	180
SEAR	22220	190
SEAR	22230	200
SEAR	22240	210
SEAR	22250	220
SEAR	22260	230
SEAR	22270	240
SEAR	22280	250
SEAR	22290	260
SEAR	33300	270
SEAR	33310	280
SEAR	33320	290
SEAR	33330	300
SEAR	33340	310
SEAR	33350	320
SEAR	33360	330
SEAR	33370	340
SEAR	33380	350
SEAR	33390	360
SEAR	44400	370
SEAR	44410	380
SEAR	44420	390
SEAR	44430	400
SEAR	44440	410
SEAR	44450	420
SEAR	44460	430
SEAR	44470	440
SEAR	44480	450
SEAR	44490	460
SEAR	55500	470
SEAR	55510	480
SEAR	55520	490
SEAR	55530	500
SEAR	55540	510
SEAR	55550	520
SEAR	55560	530
SEAR	55570	540
SEAR	55580	550
SEAR	55590	560


```

3 Y1 = G(I,J)-CRIT(NCASE,AR(I))
  Y2 = G(I,J+1)-CRIT(NCASE,AR(I))
  CALL INTERP (AI(J),AI(J+1),Y1,Y2,AIVAL)
  K = K+1
  X(K) = AR(I)
  Y(K) = AIVAL
  GO TO 5
4 K = K+1
  X(K) = AR(I)
  Y(K) = AI(J)
5 CONTINUE

      SEARCH FOR SIGN CHANGE BY ROWS AND INTERPOLATE FOR ALPHA
      REAL AT WHICH SIGN CHANGE OCCURS

      DO 10 I=1,NDIM
      DO 10 J=1,MDIM
      IF (G(J,I)-CRIT(NCASE,AR(J))) 7,9,6
      IF (G(J+1,I)-CRIT(NCASE,AR(J+1))) 8,8,10
      IF (G(J+1,I)-CRIT(NCASE,AR(J))) 10,8,8
      Y1 = G(J,I)-CRIT(NCASE,AR(J))
      Y2 = G(J+1,I)-CRIT(NCASE,AR(J+1))
      CALL INTERP (AR(J),AR(J+1),Y1,Y2,ARVAL)
      K = K+1
      X(K) = ARVAL
      Y(K) = AI(I)
      GO TO 10
9 K = K+1
  X(K) = AR(J)
  Y(K) = AI(I)
10 CONTINUE

      RETURN
      END

C ..... SUBROUTINE INTERP(X1,X2,Y1,Y2,X3) .....
C
C PURPOSE
C
C TO LINEARLY INTERPOLATE FOR THE POINT OF ACTUAL SIGN
C CHANGE (X3) BETWEEN TWO POINTS (Y1 & Y2) OF OPPOSITE
C SIGN. THE X-COORDINATES OF Y1 & Y2 ARE X1 & X2, RESPECTIVELY.
C
C SAMPLE OF THE CALLING ARGUMENT

```

```

SEAR 570
SEAR 580
SEAR 590
SEAR 600
SEAR 610
SEAR 620
SEAR 630
SEAR 640
SEAR 650
SEAR 660
SEAR 670
SEAR 680
SEAR 690
SEAR 700
SEAR 710
SEAR 720
SEAR 730
SEAR 740
SEAR 750
SEAR 760
SEAR 770
SEAR 780
SEAR 790
SEAR 800
SEAR 810
SEAR 820
SEAR 830
SEAR 840
SEAR 850
SEAR 860
SEAR 870
SEAR 880
SEAR 890
SEAR 900
SEAR 910
SEAR 920
SEAR 930

INTE 10
INTE 20
INTE 30
INTE 40
INTE 50
INTE 60
INTE 70
INTE 80
INTE 90

```



```

C      C      C
DELX = .1
C      C      C
GRAPH TITLE
C      C      C
CALL NEWPEN (2)
CALL SYMBOL(X0,Y0,HT,'STABILITY CONTOUR PLOT',0.,22)
X0 = X0+3.*DELX
YC = Y0-DELY1
CALL SYMBOL(X0,Y0,HT,'FOR THE CASE N = 0',0.,18)
C      C      C
MESH VALUE
C      C      C
CALL NEWPEN (1)
X0 = X0+4.*DELX
Y0 = Y0-DELY1
CALL SYMBOL(X0,Y0,HT1,'NMESH = ',0.,9)
CALL NUMBER (999.,999.,HT1,SN,0.,-1)
C      C      C
REY VALUE
Y0 = Y0-DELY2
CALL SYMBOL(X0,Y0,HT1,'REY = ',0.,9)
CALL NUMBER (999.,999.,HT1,SREY,0.,-1)
C      C      C
LAMBDA VALUE
YC = Y0-DELY2
CALL SYMBOL(X0,Y0,HT1,'LAMBDA = ',0.,9)
CALL NUMBER (999.,999.,HT1,SLAMDA,0.,1)
C      C      C
STABILITY AREA LABELS
NOTE - SINCE THE SHAPE OF THE CURVE VARIES WITH
      EACH SET OF INPUT DATA, THE COORDINATES OF THE FOLLOWING
      LABELS MUST BE ADJUSTED FOR EACH SPECIFIC PLOT.
C      C      C
CALL NEWPEN (2)
CALL SYMBOL (4.0,4.5,HT1,'SUPERCRITICAL',0.,13)
CALL SYMBOL (5.6,4.5,HT1,'SUBCRITICAL',0.,11)
CALL SYMBOL (6.9,4.5,HT1,'STABLE',0.,6)
YC = 4.5-DELY2
CALL SYMBOL (4.0,Y0,HT1,'INSTABILITY',0.,12)
CALL SYMBOL (5.6,Y0,HT1,'INSTABILITY',0.,11)
C      C
RETURN
END
C      C

```



```

.....
THE FOLLOWING CARDS COMPRISE THE DATA DECK FOR PROGRAM STBCONT.
/*
//GD.SYSIN DD *
.
DATA DECK FROM ONE RUN OF PROGRAM PIPEO (MODENO = 2)
.
/*
.....

```


LIST OF REFERENCES

1. Davey, A., and Drazin, P.G., "The Stability of Poiseuille Flow in a Pipe," Journal of Fluid Mechanics, v. 36, part 2, p. 209, 22 August 1968.
2. Garg, V.K., and Rouleau, W.T., "Linear Spatial Stability of Pipe Poiseuille Flow," Journal of Fluid Mechanics, v. 54, part 1, p. 113, 6 January 1969.
3. Gill, A.E., "The Least-Damped Disturbance to Poiseuille Flow in a Circular Pipe," Journal of Fluid Mechanics, v. 61, part 1, p. 765, 3 December 1973.
4. Harrison, W.F., On the Stability of Poiseuille Flow, Ae. E. Thesis, Naval Postgraduate School, Monterey, California, 1975.
5. Huang, L.M. and Chen, T.S., "Stability of Developing Flow Subject to Non-axisymmetric Disturbances," Journal of Fluid Mechanics, v. 63, part 1, p. 183, 16 April 1973.
6. Johnston, R.H. III, A Program for the Stability Analysis of Pipe Poiseuille Flow, M.S. Thesis, Naval Postgraduate School, Monterey, California, 1976.
7. Leite, R.J., An Experimental Investigation of Axially Symmetric Poiseuille Flow, Report No. OSR-TR-56-2, Air Force Contract AF18(600)-350, November, 1956.
8. Naval Postgraduate School Report NPS-67Gn77051, Improved Finite Difference Formulas for Boundary Value Problems, by T.H. Gawain and R.E. Ball, 1 May 1977.
9. Naval Postgraduate School Report NPS67-78-006, A Basic Reformulation of the Pipe Flow Stability Problem and Some Preliminary Numerical Results, by T.H. Gawain, 1 September 1978.
10. Reynolds, O., "An Experimental Investigation of the Circumstances which Determine whether the Motion of Water Shall be Direct or Sinuous, and the Law of Resistance in Parallel Channels," Phil. Trans. Royal Soc., 174, p. 935-982, 1883.
11. Salwen, H., and Grosch, C.E., "The Stability of Poiseuille Flow in a Pipe of Circular Cross-section," Journal of Fluid Mechanics, v. 54, part 1, p. 93, 6 March 1972.

INITIAL DISTRIBUTION LIST

	No. Copies
1. Defense Documentation Center Cameron Station Alexandria, Virginia 22314	2
2. Library, Code 0142 Naval Postgraduate School Monterey, California 93940	2
3. Department Chairman, Code 67 Department of Aeronautics Naval Postgraduate School Monterey, California 93940	1
4. Prof. T.H. Gawain, Code 67Gn Department of Aeronautics Naval Postgraduate School Monterey, California 93940	5
5. LT Michael James Arnold, USN 10825 Single Tree Lane Spring Valley, California 92077	1

Thesis
A7259
c.1

Arnold

Investigation of
pipe flow instability
and results for wave
number zero.

179850

T
A
C

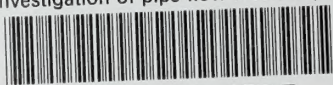
Thesis
A7259
c.1

Arnold

Investigation of
pipe flow instability
and results for wave
number zero.

179850

Investigation of pipe flow instability a



3 2768 002 01257 7
DUDLEY KNOX LIBRARY